Technical report on a visit to The Radiation Laboratory at the University of Michigan

by

Leonard Rexberg, Ph.D.

University of Michigan
Radiation Laboratory
NASA/Center for Space Terahertz Technology
3238 EECS Building
Ann Arbor, MI 48109-2122
U.S.A.

Solstralegatan 44
417 42 Gothenburg
SWEDEN

December 1991

Preface

The microwave work made in the U.S. has a large potential compared to the microwave industry in Europe. This is also reflected in the research activity at the major Universities such as UCLA, Michigan and Massachussets. Sweden, for example, has only activities going on at Ericsson Radar Electronics, Bofors Electronics in Stockholm and at Chalmers University of Technology in Gothenburg. Some other minor companies also have activities in this area, but they are often working on the application level not on basic research. Further, the Swedish industry is interested in keeping good relations with people in the U.S. who are currently working in this area. Therefore, it is important that an exchange of knowledge and personal contacts can be established between the two countries. In this spirit I have received a research grant from the Royal Swedish Academy of Sciences in order to perform microwave research in the U.S.

I applied for the grant in September 90 and received 40.000 SEK from the academy in December. As I by that time not yet had a confirmed affiliation with a host University in the U.S. I did not transfer the grant to my account until August 91. I had received a confirmation in July from the University of Michigan to perform research in the fall of -91. Until then I had been working as a postdoc at the Division of Network Theory since the defense of my Ph.D. thesis in April. During this time I worked on frequency scanning grating reflector antennas together with Dr. Stefan Johansson who is now working with the Ericsson company in Gothenburg. I also did a minor work on reflector-antennas in cooperation with Professor Per-Simon Kildal at the Network Division.

My work at the Radiation Laboratory at the University of Michigan concerned research on a new type of transmission lines suitable for feeding conformal antennas. The transmission line consists of a pair of parallel slots which can be excited in the 'odd' or in the 'even' mode. Using the 'odd' mode makes the transmission line radiate less compared to conventional transmission lines. In addition, when a cavity is placed under the transmission line the radiation is further decreased. The cavity is designed to be working under cut off so that only the fundamental mode is propagating along the two slots. The metal strip between the slots is suspended on a thin membrane with low losses. The whole structure then has very small losses compared to conventional designs.

The Radiation Laboratory at University of Michigan.

The Radiation Laboratory started out as the Upper Atmospheric Physics Section of the Michigan Aeronautical Research Center in 1948, and assumed its present name when it became part of the Electricl Engineering Department of the College of Engineering in 1957. The initial focus of research was in radar cross sections, and this soon expanded to include all matters concerned with the radiation, propagation, and scattering of electromagnetic waves. Scattering by all types of targets has continued to be a main topic of research, but other areas which are now emphasized are electromagnetic interference, microstep and printed circuit antennas, and the remote sensing of terrain and vegetation [1].

Abstract

This report presents and summarizes the technical research made at the University of Michigan, Radiation Laboratory, by Leonard Rexberg during a three months visit. The research deals with a new type of monolithic transmission lines characterized by low loss, low radiation and good abillity to conformally feed planar antennas. It consists of a cavity-backed double slot-line and having free space on the other side. The cavity is designed to work under cut off so that only the fundamental mode can propagate in the slot aperture. This feed line is called microshield-line and was invented by the researchers at the Radiation Laboratory.

In this work the new transmission line is used as a feed for planar slot antennas. The two feed slots are bended apart to form a kind of loop antenna wich when designed properly in size will radiate a broadside radiation pattern. Different parts of the loop may be excited in phase when the feed line is excited in the 'even' or 'odd' modes. Also dipole slot antennas are possible radiators. The antenna design is applicable at sub-mm frequencies using membrane technology on for example Silicon or GaAs substrates. Normalized input impedance and radiation patterns show the performance of the new antenna.

Acknowledgements

I would like to thank my new friends at the Radiation Laboratory for making my three month stay a very pleasent one. Especially I want to thank Prof Linda Katehi who gave me a great deal of inspiration during my work and had very good suggestions on interesting research topics. Finally I am happy that I met such wonderful people as Prof Gabriel Rebeiz, Prof Emeritus Chen-To Tai, Emilie van Deventer, Nihad Dib, Valid Ali-Ahmad, George Eleftheriades, Hans Ekström and Steven Gearhart. There are also other very kind people who have helped me during my stay at the Radiation Laboratory whom I would like to thank.

This work was finacially supported by "The Royal Swedish Academy for Sciencies" by a 40.000 SEK grant for microwave research in the USA.

Contents

List of Figures

1 Introduction

The microshield line is a new type of monolithic transmission line that is appropriate for circuit or array antenna applications [2]. It consists of two narrow parallel slits cut in an infinite ground plane and shielded on the other side by a waveguide or cavity of metalized walls. The two slits can be excited either in the 'even' mode or in the 'odd' mode depending on the desired characteristics. The dimensions of the shielding structure on the back side are designed to assure a cut-off frequency that is higher than the operating frequency. Thereby we are sure that only the fundamental mode is propagating along the slit apertures. Such a structure can be made monolithically using etching and metal deposition techniques. Furthermore, the inner conductor between the two slits can be suspended in air by using membrane technology [3].

The membrane technology has already sucessfully been used to obtain array antennas operating at millimeter-wave frequencies as high as 2.5 THz [4]. Power losses which can be very severe at high frequencies can be nearly eliminated by this technique. The membranes have until now been fabricated on silicon substrates but the Radiation Laboratory is currently working on achieving the same goals with GaAs compounds. The microshield line is also suitable to feed planar microwave antennas since the radiation from the feed when operated in the odd mode is extremly low [2]. That is, unwanted spurious radiation can be eliminated or minimized to a low level. The antenna itself can be forced to radiate by bending the slits to form for example a rectangular loop antenna mounted in an infinite ground plane. Two sides will then be operating in the 'even' mode and the other two will operate in the 'odd' mode. The even mode excitation will give rise to an in-phase radiation while the other two will cause an unwanted cross-polarisation. Alternatively, the 'even' mode excitation can be used to obtain dual and circular polarisation.

The advantages using the microshield line with a membrane suspended center conductor are characterized by low spurious radiation and the ability to operate without the need for via-holes or the use of air-bridges for ground equalization. Furthermore, a wide range of impedances may be achieved by varying the size of the microshield waveguide dimensions. In addition, the effective propagation factor in the slits are almost the same as in free space as long as the distance to the nearest waveguide wall is kept large enough. This is usually a built-in feature of the microshield line since one wants to keep the distance between the slits as short as possible to avoid radiation.

This report deals with the theoretical study of loop antennas that are excited by the microshield line. The loops are rectangular in order to be easy to model using rectangular basis functions for the approximation of the magnetic current in the slits. Two types of antennas are tested: the microshield-line fed antenna and the ordinary coplanar waveguide (CPW) fed antenna. Thesse two antennas can be joined into one antenna suitable for direct-on-antenna mixing between the RF-signal and a LO-signal. A simple version using a pair of connected slot antennas [5] printed on a dielectric slab has previously been presented and shows good radiation performance and isotropic conversion

loss. This integrated technique is also suggested for the cavity-backed microshield-line fed loop antenna. Also the possibility to obatin circular radiation simultaneously using the microshield line and the CPW is discussed.

2 The object of the research project.

The object of the research project is to find out how to feed planar antennas by using the new microshield line. Let us start by discussing some various shapes of the microshield-line fed antenna. The microshield-line itself is depicted in a top view in Figure 1. The distance W between the two slits should be kept small so that the transmission line does not radiate. When the two slits are excited in the 'odd' mode there will be a cancellation of the field strength in the broadside direction. Further out there will of course be som spurious radiation. This radiation is in general transverse to the desired direction of the radiation. So, properly designed, an antenna fed by this transmission line would show relatively low cross-polarisation.

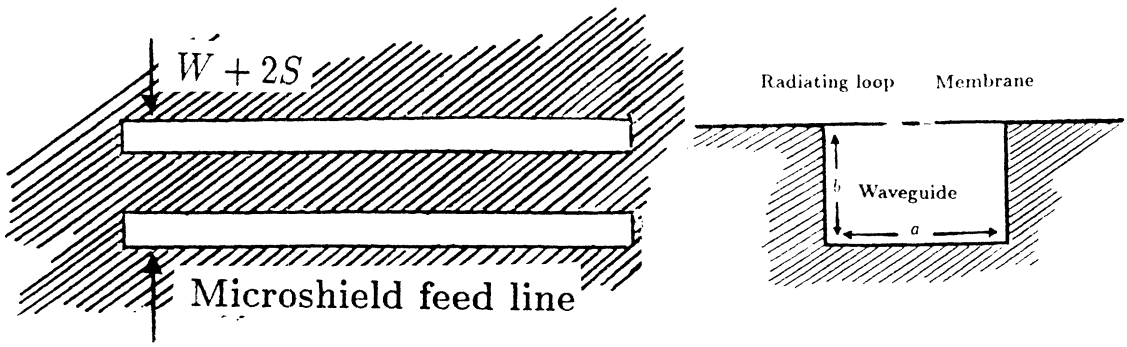

Figure 1: The parallell two slits forming a microshield line. The microshield line is backed by a cavity on the other side.

Figure 2 shows a dipole slot antenna that is excited by the new microshield line. It is noted that if the two slits in the transmission lines are excited in the 'odd' mode there will be an in-phase 'even' mode excitation of the two dipole arms. Hence, the antenna will radiate a broadside pattern having a broad E-plane cut and a somewhat narrower H-plane-cut. The H-plane cut has to go to zero at $\theta = 0°$ and $\theta = 180°$ because of the boundary conditions of the tangential electric field on the surface of the surrounding ground plane. The radiation in the back-direction is blocked by the cavity so that it only radiates on one side of the antenna.

The second antenna to study is depicted in Figure 3. It shows the microshield line feeding a loop antenna which will give a slightly higher gain than the single slot dipole. The length of the loop is chosen to be $\lambda/2$. This antenna can be viewed as consisting of two slot antennas working in phase at a distance of about $0.2 - 3\lambda$ apart. The two other arms in the transverse direction to the radiating slots will be out-of-phase to each other. These two arms will probably increase the cross-polar radiation coming from the

feed line. This is because of the larger distance bewteen the arms. One way to avoid the crosspolarisation is to make the loop larger thus increasing the in-phase radiation in favour of the unwanted cross-polarization.

The electrci field in the slots of the antenna and feed line is calculated from Maxwell's equations by transforming them (moment method) into a linear set of matrix equations. Solving the matrix equation gives the amplitudes of the basis functions forming the electric field. The field is expanded in a series of rooftop functions as depicted in Figure 4. The antenna is excited by gap generators which are represented by placing a '1' in the appropriate position in the right hand side vector of the matrix equation.

The voltage standing wave ratio (VSWR), and hence the input impedance and reflection coefficient, can be calulated by plotting the magnitude of the total current on the feed line. Taking the ratio of the top value to the minimum value then gives the standing wave ratio (See Appendix A). The next thing to do is to calculate the phase of the reflection coefficient by measuring the distance of the first maximum from the reference plane. We know that the phase of the reflection coefficient is zero at a maximum of the standing wave, and further we know that the distance between two maxima is exactly half a wavelength of the particular medium. This therefore gives the phase of the reflection coefficient. Problems may arise if the standing wave form of the total current does not show a typical periodic pattern. Then we have to extend the feed line in order to make shure that the current has settled down. This is yet to be investigated.

It is worthwhile to mention that the total current can easily be plotted by just plotting the amplitude coefficients and then connect them with straight lines. We remember that the rooftop functions are placed to overlap in such a way that the amplitude at the edge of one function is zero whlie the amplitude of the next current element is maximum. In between these two points the current is linear.

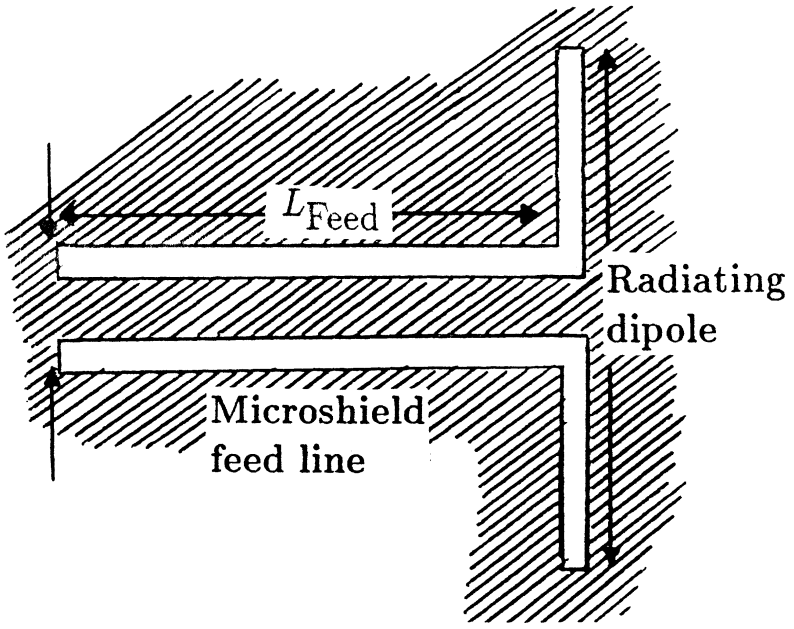

Figure 2: A slot dipole antenna which is excited by the new microshield transmission line. The two slits forming the feed are out-of-phase while the two arms of the dipole are in-phase.

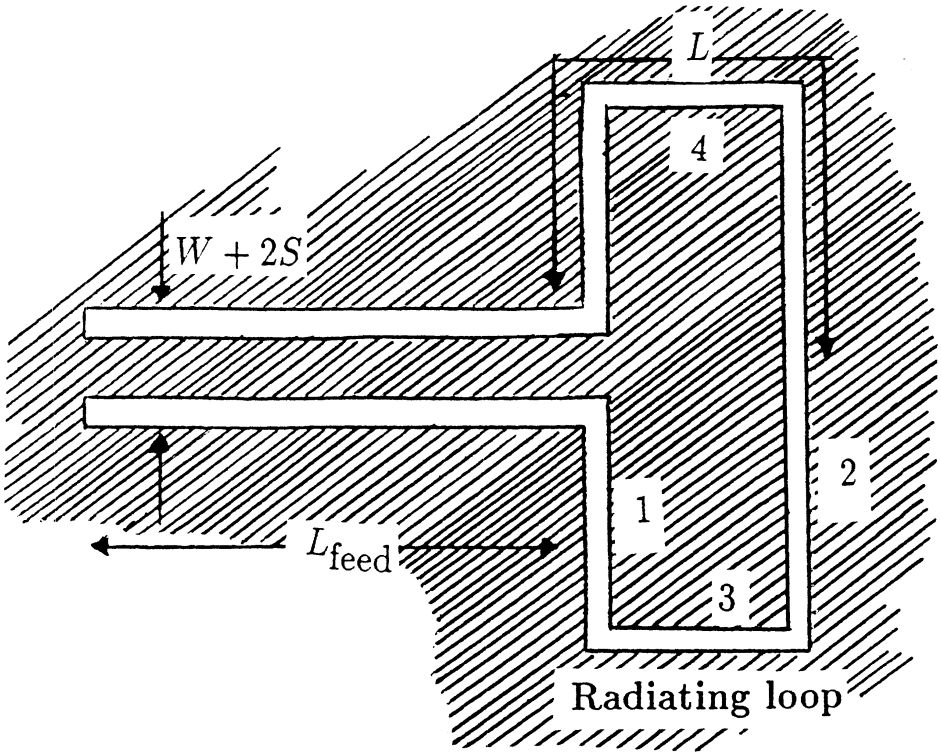

Figure 3: A slot loop antenna fed by the new microshield line. The two slits forming the transmission line are excited out-of-phase whereas the two oppositely directed arms of the dipole are radiating in phase.

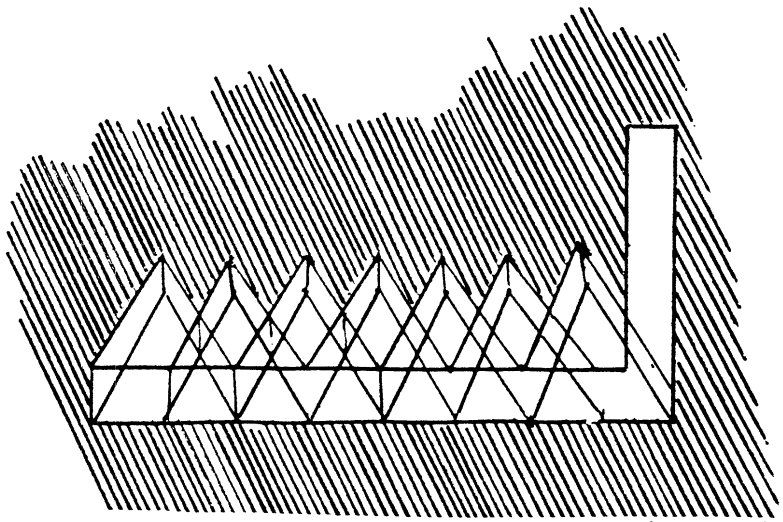

$$\vec{J}_n^{PWS}(x,z) = \frac{1}{W_f}\frac{\sin\left[k_e(h-|z-z_n|)\right]}{\sin k_e h}\hat{z}\text{for}\begin{cases}|z-z_n| < h\\ |x| < W_f/2\end{cases}$$

Figure 4: Rooftop basis functions in the slots forming the electric field. The amplitudes of the basis functions are solved by applying the method of moments to Maxwell's equations.

3 Analysis

The analysis of the structure is performed using techniques referred to as spectral domain techniques. This basically means that the two-dimensional Fourier transform is applied to Maxwell's equations and then these equations in turn are split into a pair of transverse electric (TE) and transverse magnetic (TM) equations. This especially simplifies the analysis when different dielectric layers are to be included into the analysis. Each new layer is then represented by a cascade matrix which is multiplied in a chain-wise manner to the starting configuration. This can be done automatically in a computer program which is easy to modify to meet the geometry of new structures. The following sections gives a brief discussion of the equivalent network calculations.

3.1 The electric field from a planar current source located in a stratified dielectric medium. External field problem.

Before we can solve the electric field in a particular region we must first determine the induced magnetic and electric currents. This can for example be done by approximating the unknown currents in a finite series of known basis functions with unknown coefficients. These coefficients are then solved by for example applying the method of moments to some integral equation formed by the boundary conditions for the field. A short presentation is given later in this report. If we deal with a slot in a ground plane then we can apply Schellkunoff's equivalence principle and imaging techniques to reduce the original problem. The result will be just a magnetic current (no electric current) radiating into the structure. This is the case because the electric currents will be short-circuited by the ground plane. The integral equation for a slot in a ground-plane dividing two regions is given by the following identity:

$$\vec{H}_{1t}^{scat}(x,z) - \vec{H}_{2t}^{inc}(x,z) = \vec{H}_{t}^{inc}(x,z) \tag{1}$$

where the indeces (1) and (2) refer to the two regions. The equation above forces the tangential magnetic field on opposite sides of the slot to be equal. In this report we deal with planar electric or magnetic antennas which are placed within a stratified dielectric structure. According to Schellkunoff's equivalence priciple we therefore need to calculate the tangential electric field produced by a specific planar current source placed at a given arbitrary position in the stratified dielectric structure. In the early papers based on the moment method solutions, the magnetic vector potential approach was used to calculate the tangential electric field. The magnetic vector potentials in the dielectric slabs and in the free space region have to be matched at the interfaces in order to satisfy the boundary conditions. Therefore, a set of linear equations has then to be

solved analytically in order to find the correct expression for the field in the spectral domain. Obviously, the number of equations will rapidly increase as more dielectric layers are included. This will lead to complicated calculations. So, we need a simpler approach to deal with stratified structures.

A better technique, frequently used in network theory, is based on transmission line equivalent circuits. These are derived directly from Maxwell's equations by separating them into the transverse and longitudinal parts. The transverse part is then in turn split into one transverse magnetic (TM) and one transverse electric (TE) part with appropriate coefficients. These scalar coefficients each satisfy the TM- and TE transmission line equations. Each dielectric layer section is represented by a cascade matrix relating the load voltage and current to the corresponding input excitation.

The electromagnetic boundary conditions are transferred to the fundamental current and voltage laws that where formulated by Kirchhoff. An overall matrix for the stratified medium can then be found by a straight forward network analysis. This matrix can be used to calculate the interactions between currents on the same dielectric layer as well as on other layers. The detailed derivations of the planar electric source radiation in a layered medium has been presented in Reference 7. Therefore, the results will only be rephrased in this report and then applied to a double layer microstrip antenna.

3.2 The transverse magnetic field expressed by means of equivalent TM- and TE- scalar currents in the spectral domain.

The electric and magnetic field transverse (i.e. in the xz-plane) to the direction of propagation can as mentioned be decomposed into one TM- part and one TE-part. This procedure will in turn leave two scalar differential transmission line equations each for the coefficients of the transverse vectors [7]. The coefficients can be viewed as a voltage and a current corresponding to the electric and magnetic field respectively. These equations can then be solved by applying basic electromagnetic boundary conditions. The boundary conditions state that the electric field must be continuous across two different media while the magnetic field is discontinuous across any electric current source in the structure. In addition, the electric field tangential to any conducting surface must vanish. If there is no electric current present, then the magnetic tangential field must also be continuous. These boundary conditions also hold for the scalar coefficients. The voltage in the interface between two circuits must be equal and the current is discontinuous whereever a current source is present. So, the original electromagnetic problem is readily transformed into an equivalent network problem from which all field components may be solved. We start by defining the transverse electric field by means of the transverse vector eigenfunctions, as:

$$\vec{H}_t(x,y,z) = \int_{-\infty}^{+\infty}\int_{-\infty}^{+\infty} \left[I_{TM}(k_x,y,k_z)\vec{h}_t^{\,TM}(k_x,k_z) + I_{TE}(k_x,y,k_z)\vec{h}_t^{\,TE}(k_x,k_z) \right] dk_x dk_z \qquad (2)$$

As mentioned, the TM- and TE-currents $[I_{TM}(k_x,y,k_z)$ and $I_{TE}(k_x,y,k_z)]$ satisfy the scalar transmission line equations which are obtained from the Maxwell's equations when splitting into TE and TM components [7]. These transmission line equations are:

$$-\frac{\partial}{\partial y} V_{TM,TE}(k_x,y,k_z) = jk_y Z_c^{TM,TE} I_{TM,TE}(k_x,y,k_z) \qquad (3)$$

$$-\frac{\partial}{\partial y} I_{TM,TE}(k_x,y,k_z) = jk_y Y_c^{TM,TE} V_{TM,TE}(k_x,y,k_z) \qquad (4)$$

where the characteristic line impedances Z_c^{TM} and Z_c^{TE} are defined by:

$$Z_c^{TM} = \frac{1}{Y_c^{TM}} = \frac{k_y}{\omega\varepsilon_r\varepsilon_0} \qquad (5)$$

$$Z_c^{TE} = \frac{1}{Y_c^{TE}} = \frac{\omega\mu}{k_y} \qquad (6)$$

The spectral domain propagation factor k_y, in the y-direction normal to the antenna surface, satisfies the separation equation in the specific region defined by a dielectric constant ε_r, as:

$$k_y^2 = \epsilon_r k_0^2 - k_x^2 - k_z^2 \qquad (7)$$

The vectors $\vec{h}_t^{\,TM}$ and $\vec{h}_t^{\,TE}$ in Eq. (2) are the transverse vector eigenfunctions in the k_xk_z-plane. These are orthogonal to each other and are expressed in terms of plane waves with appropriate vector coefficients, as [7]:

$$\vec{h}_t^{\,TE}(k_x,k_z) = \frac{1}{\sqrt{k_x^2 + k_z^2}} \left(k_z\hat{z} + k_x\hat{x}\right) e^{-j(k_x x + k_z z)} \qquad (8)$$

$$\vec{h}_t^{TM}(k_x, k_z) = \frac{1}{\sqrt{k_x^2 + k_z^2}} (-k_x \hat{z} + k_z \hat{x}) \, e^{-j(k_x x + k_z z)} \tag{9}$$

The factor $\sqrt{k_x^2 + k_z^2}$ in Eqs. (8) and (9) accounts for the normalisation of the vectors. If these definitions are inserted into Eq. (2) we end up with a formula expressing the tangential components of the electric field in terms of the spectral domain voltage along the line, according to:

$$H_z(x, y, z) = \int_{-\infty}^{+\infty} \int_{-\infty}^{+\infty} \tilde{H}_z(k_x, y, k_z) \, e^{-j(k_x x + k_z z)} \, dk_x dk_z \tag{10}$$

$$H_x(x, y, z) = \int_{-\infty}^{+\infty} \int_{-\infty}^{+\infty} \tilde{H}_x(k_x, y, k_z) \, e^{-j(k_x x + k_z z)} \, dk_x dk_z \tag{11}$$

where the Fourier transform of the magnetic field components are expressed by a superposition of the equivalent TM- and TE-currents $I_{TM}(k_x, y, k_z)$ and $I_{TE}(k_x, y, k_z)$, as:

$$\tilde{H}_z(k_x, y, k_z) = \frac{-I_{TM}(k_x, y, k_z) k_x + I_{TE}(k_x, y, k_z) k_z}{\sqrt{k_x^2 + k_z^2}} \tag{12}$$

$$\tilde{H}_x(k_x, y, k_z) = \frac{I_{TM}(k_x, y, k_z) k_z + I_{TE}(k_x, y, k_z) k_x}{\sqrt{k_x^2 + k_z^2}} \tag{13}$$

Now, it remains to calculate these currents in terms of the current source for both TM- and TE-propagation. In the next section we will present a network tool that is suitable when the source is radiating into a stratified dielectric medium.

3.3 The scalar TE- and TM-currents in the spectral domain in terms of the equivalent two-port matrices.

It is useful to introduce two-port impedance and cascade matrices when treating structures in several layers. These are then used to calculate the currents $I_{TM}^{(1,2)}(kx, y, k_z)$ or

MISSING
PAGE

Consider the slot radiating into a dielectric slab of thickness 'd' in Figure 6. We only consider one of the two half spaces since the other can be treated in an analogeous way. According to the foregoing discussion the dielectric slab can be treated by an equivalent transmission line. The transmission line is excited by a voltage source which is placed in the location of the aperture plane. This circuit represents both TM and TE propagation, so the characteristic line impedances must be chosen in view of Eqs. (5) and (6). The equivalent two-port network is obtained by multiplying the transmission line T-matrix with the T-matrix of the free space load matrix.

The equivalent two-port circuit is composed of two parts, namely: the cascade matrix for the spacing sheet between the layers (T_1) and the free space impedance (T_2) cascade matrix. The cascade matrix for the dielectric sheet is obtained as:

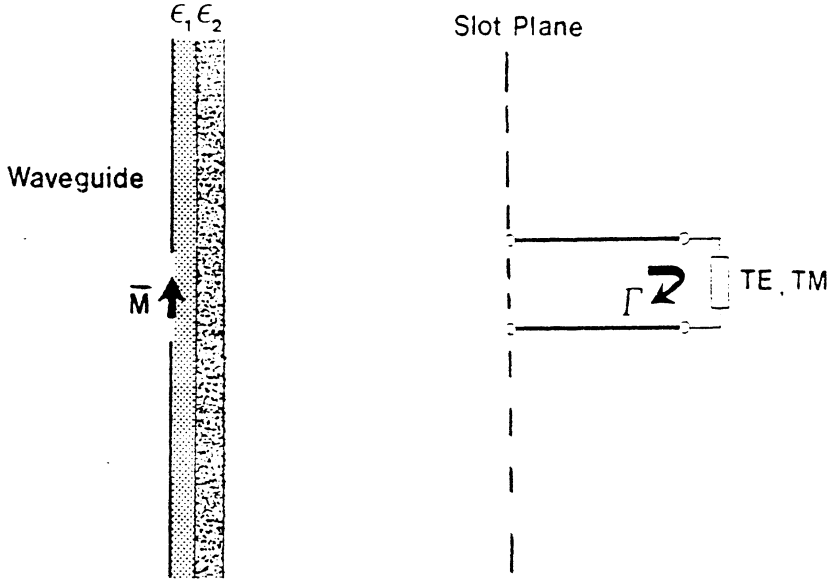

Figure 6: A slot radiating into a dielectric slab and its equivalent transmission line circuit in the Fourier domain.

$$T_1 = \begin{bmatrix} \cos(k_{1y}d_1) & jZ_{c_1}^{TM,TE}\sin(k_{1y}d_1) \\ jY_{c1}^{TM,TE}\sin(k_{1y}d_1) & \cos(k_{1y}d_1) \end{bmatrix} \tag{17}$$

where d_1 is the thickness of the dielectric layer. The cascade matrix for the free space load admittance $Y_{c2}^{TM,TE}$ is given by:

$$T_2 = \begin{bmatrix} 1 & 0 \\ Y_{c2}^{TM,TE} & 1 \end{bmatrix} \tag{18}$$

The characteristic line admittances and impedances for the two regions are obtained from Eqs. (5) and (6), as:

$$Y_{ci}^{TM} = \frac{\omega \varepsilon_{ir} \varepsilon_0}{k_{iy}} \qquad i = 1,2 \tag{19}$$

$$Y_{ci}^{TE} = \frac{k_{iy}}{\omega \mu} \qquad i = 1,2 \tag{20}$$

$$k_{iy} = \sqrt{\varepsilon_{ir} k_0^2 - k_x^2 - k_z^2} \qquad i = 1,2 \tag{21}$$

The total matrix is then obtained by a cascade multiplication of T_1 and T_2 as:

$$T_{tot}^{TM,TE} = T_1^{TM,TE} T_2^{TM,TE} = \begin{bmatrix} A_{tot}^{TM,TE} & B_{tot}^{TM,TE} \\ C_{tot}^{TM,TE} & D_{tot}^{TM,TE} \end{bmatrix} \tag{22}$$

So, if the transmission line voltage at a given y-plane is known, one has all the information needed for the evaluation of the electric/magnetic field at that plane.

3.4 The transverse electric field components in terms of the electric filed in the slot antenna.

Having calculated the equivalent two-port network we can derive the tangential magnetic field by finding the TE and TM currents at the input and output ports. In this case the output port is open. These currents are related to the input excitations as given below by Eqs. (23) and (24):

$$\begin{bmatrix} I_{TM}^{(1)}(k_x, k_z) \\ I_{TM}^{(2)}(k_x, k_z) \end{bmatrix} = \begin{bmatrix} Y_{11}^{TM}(k_x, k_z) & Y_{12}^{TM}(k_x, k_z) \\ Y_{21}^{TM}(k_x, k_z) & Y_{22}^{TM}(k_x, k_z) \end{bmatrix} \cdot \begin{bmatrix} M_{TM}^{(1)}(k_x, k_z) \\ M_{TM}^{(2)}(k_x, k_z) \end{bmatrix} \tag{23}$$

$$\begin{bmatrix} I_{TE}^{(1)}(k_x, k_z) \\ I_{TE}^{(2)}(k_x, k_z) \end{bmatrix} = \begin{bmatrix} Y_{11}^{TE}(k_x, k_z) & Y_{12}^{TE}(k_x, k_z) \\ Y_{21}^{TE}(k_x, k_z) & Y_{22}^{TE}(k_x, k_z) \end{bmatrix} \cdot \begin{bmatrix} M_{TE}^{(1)}(k_x, k_z) \\ M_{TE}^{(2)}(k_x, k_z) \end{bmatrix} \tag{24}$$

where:

$$\begin{bmatrix} Y_{11}^{TM,TE} & Y_{12}^{TM,TE} \\ Y_{21}^{TM,TE} & Y_{22}^{TM,TE} \end{bmatrix}^{-1} = \frac{1}{C_{tot}^{TM,TE}} \begin{bmatrix} A_{tot}^{TM,TE} & \Delta T_{tot}^{TM,TE} \\ 1 & D_{tot}^{TM,TE} \end{bmatrix} \tag{25}$$

where:

$$\Delta T = A_{tot}^{TM,TE} D_{tot}^{TM,TE} - B_{tot}^{TM,TE} C_{tot}^{TM,TE} \tag{26}$$

The impedance matrices in the foregoing equations are found by using Eqs. (16) - (22). The TE and TM currents $M_{TE}^{(1,2)}$ and $M_{TE}^{(1,2)}$ in Eqs. (23) and (24) are related to the Fourier transform of the magnetic currents according to Eqs. (27) and (28) below:

$$\begin{bmatrix} M_{TE}^{(1)}(k_x, k_z) \\ M_{TM}^{(1)}(k_x, k_z) \end{bmatrix} = \frac{1}{4\pi^2} \frac{1}{\sqrt{k_x^2 + k_z^2}} \begin{bmatrix} k_x & k_z \\ k_z & -k_x \end{bmatrix} \begin{bmatrix} \tilde{M}_x^{(1)}(k_x, k_z) \\ \tilde{M}_z^{(1)}(k_x, k_z) \end{bmatrix} \tag{27}$$

and

$$\begin{bmatrix} M_{TE}^{(2)}(k_x, k_z) \\ M_{TM}^{(2)}(k_x, k_z) \end{bmatrix} = \frac{1}{4\pi^2} \frac{1}{\sqrt{k_x^2 + k_z^2}} \begin{bmatrix} k_x & k_z \\ k_z & -k_x \end{bmatrix} \begin{bmatrix} \tilde{M}_x^{(2)}(k_x, k_z) \\ \tilde{M}_z^{(2)}(k_x, k_z) \end{bmatrix} \tag{28}$$

The spectral domain currents $\tilde{M}_x^{(1,2)}(k_x, k_z)$ and $\tilde{M}_z^{(1,2)}(k_x, k_z)$ on the right hand side in turn are related to the magnetic currents by:

$$\tilde{M}_{x,z}^{(1,2)}(k_x, k_z) = \int_{-\infty}^{+\infty} \int_{-\infty}^{+\infty} M(x, z)_{x,z}^{(1,2)} \, e^{+j(k_x x + k_z z)} \, dx dz \tag{29}$$

or in terms of the electric field in the slot:

$$\tilde{M}_{x,z}^{(1,2)}(k_x, k_z) = -\hat{n} \times \int_{-\infty}^{+\infty}\int_{-\infty}^{+\infty} E(x,z)_{x,z}^{(1,2)}\, e^{+j(k_x x + k_z z)}\, dxdz \tag{30}$$

Then, according to the law of superposition, one readily finds the total field at the location of the two slots as the sum of the partial contributions from the two currents. This is made by means of using the transfer function implicitly given in Eqs. (23) and ,(24). Note, that the second magnetic current $M_{TM,TE}^{(2)}$ is not present in a single slot case radiating into free space. Further, the two dielectric constants for the transmission line and the free space load are equal. So in other words, the transmission line can be ommitted since it is matched by the load.

3.5 The internal field problem.

The internal field can be derived in the same manner as the external field by using image techniques. A current ribbon inside a waveguide (or in the wall of the waveguide) can be treated in free space as if it were a periodic current. Now, periodic currents can be expanded in their Fourier series which will give a series of Dirac delta functions. Inserting this train of Dirac functions in the field expression derived above will have the effect of sampling the integrand at a number of points determined essentially by the waveguide modes. Both propagating and non-propagating modes has to be taken into account. Let us explain this with some equations. Consider the slot element cut in the broad face of a waveguide as depicted in Figure 7. The walls can be taken away if the equivalent magnetic current in the slot is compensated by a periodic current that is also depicted in the same figure.

The magnetic current actually consists of two series functions having the same periodicity but having a phase difference. The periodic current can be written as:

$$M(x,z) = \sum_{n=-\infty}^{+\infty} M_0(x - n2a - x') + M_0(x - n2a + x') \tag{31}$$

Now, taking the x-Fourier transform of this periodic function we obtain:

$$\int_{-\infty}^{+\infty} M(x,z)\, e^{+jk_x x}\, dx = \int_{-\infty}^{+\infty} \sum_{n=-\infty}^{+\infty} M_0(x - n2a - x') + M_0(x - n2a + x')\, e^{+jk_x x}\, dx =$$

$$= 2\cos(k_x x')\tilde{M}_0(k_x) \sum_{n=-\infty}^{+\infty} e^{jk_x n2a} \tag{32}$$

This last result is a periodic function in itself which can be seen as a complex Fourier series with equal amplitudes on each component. Now, this Fourier series must be a pulse-train of Dirac delta functions. That is, it can be written as:

$$\int_{-\infty}^{+\infty} M(x,z)\, e^{+jk_x x}\, dx = \int_{-\infty}^{+\infty} \sum_{n=-\infty}^{+\infty} M_0(x - n2a - \frac{x'}{2}) + M_0(x - n2a + \frac{x'}{2})dx =$$

$$= 2\cos(k_x x')\frac{\pi}{2a}\tilde{M}_0(k_x) \sum_{n=-\infty}^{+\infty} \delta(k_x - \frac{n\pi}{a}) \tag{33}$$

Now, this is the current that we have to insert into the fre space expressions for the magnetic and electric field. These expressions involve a Fourier transform themselves so the result will be that the integrand i sampled at regular points leaving only the summation. That is, when taking only one direction (x) into account we obtain:

$$\int_{-\infty}^{+\infty} \tilde{Q}(k_x)\tilde{M}(k_x)e^{-jk_x x}dk_x =$$

$$= \frac{\pi}{a} \sum_{n=-\infty}^{+\infty} \cos\frac{n\pi x'}{a}\, \tilde{Q}(\frac{n\pi}{a})\, \tilde{M}(\frac{n\pi}{a})\, e^{-j\frac{n\pi}{a}x} \tag{34}$$

We see that the integrand is sampled at distinct regular intervals exactly where the waveguide modes in the spectrum appear. If the waveguide is closed at the other two ends of the waveguide then we can perform the same imaging technique in the z-direction Figure 8. Only, this time the magnetic current is perpendicular to the waveguide mode. So, now we have to subtract the two periodic currents instead of adding them. This will lead to a sine-function for the displacement z' instead of a cosine-factor. We will leave this to the reader to verify.

Now, going back to the equations for the Fourier transform of the tangential H-field we can re-write them in terms of the input impedance which is seen by the slot looking into the stratified medium. Rephrasing the equations, we obtain:

$$\tilde{H}_z(k_x, y, k_z) = \frac{-I_{TM}(k_x, y, k_z)k_x + I_{TE}(k_x, y, k_z)k_z}{\sqrt{k_x^2 + k_z^2}} \tag{35}$$

$$\tilde{H}_x(k_x, y, k_z) = \frac{I_{TM}(k_x, y, k_z)k_z + I_{TE}(k_x, y, k_z)k_x}{\sqrt{k_x^2 + k_z^2}} \tag{36}$$

and inserting the input impedance we get the modified expression:

$$\tilde{H}_z(k_x, y, k_z) = \frac{-M_{TM}(k_x, y, k_z)Y_{IN}^{TM}k_x + M_{TE}(k_x, y, k_z)Y_{IN}^{TE}k_z}{\sqrt{k_x^2 + k_z^2}} \tag{37}$$

$$\tilde{H}_x(k_x, y, k_z) = \frac{M_{TM}(k_x, y, k_z)Y_{IN}^{TM}k_z + M_{TE}(k_x, y, k_z)Y_{IN}^{TE}k_x}{\sqrt{k_x^2 + k_z^2}} \tag{38}$$

Looking into the waveguide we only see a shorted transmission line with the characteristic impedance $Y_c^{TM,TE}$. However, we write down the general expressions when there is an impedance boundary on the other side of the slot. Transforming the surface boundary impedances Z^{LSM} and Z^{LSE} to the slot aperture vi obtain:

$$Y_{IN}^{TM} = Y_c^{TM} \frac{Z_c^{TM} + jZ^{LSE} \tan k_y d}{Z^{LSE} + jZ_c \tan k_y d} \tag{39}$$

$$Y_{IN}^{TE} = Y_c^{TE} \frac{Z_c^{TE} + jZ^{LSM} \tan k_y d}{Z^{LSM} + jZ_c^{TE} \tan k_y d} \tag{40}$$

where the characteristic impedances are:

$$Y_{ci}^{TM} = \frac{\omega \varepsilon_{ir} \varepsilon_0}{k_{iy}} \qquad i = 1, 2 \tag{41}$$

$$Y_{ci}^{TE} = \frac{k_{iy}}{\omega \mu} \qquad i = 1, 2 \tag{42}$$

$$k_{iy} = \sqrt{\varepsilon_{ir} k_0^2 - k_x^2 - k_z^2} \qquad i = 1, 2 \tag{43}$$

and

$$k_x = \frac{n\pi}{a} \tag{44}$$

$$k_z = \frac{m\pi}{L} \tag{45}$$

$$\tag{46}$$

where a and L are the width and length of the cavity respectively. We insert the characteristic admittances in the equations for the input admittances and obtain:

3.6 Schellkunoff's equivalence principle applied to a slot in an infinite ground plane.

In this subsection we will describe how we can make use of the Schellkunoff equivalence principle to calculate the field from a slot in an infinite ground plane. The equivalence principle can be used in many ways but only one of them will be treated here. The slot may be covered by dielectric layers or even radiate into a waveguide. Now, consider the slot in Figure 9 radiating into the dielectric slab and then into free space. According to the Schellkunoff equivalence principle we may substitute the tangential electric and magnetic field by equivalent electric and magnetic currents that are also tangential to the same surface (Figure 10). These currents are related to the field on both sides of the interface as:

$$\vec{J}_s = \hat{n} \times (\vec{H}_1 - \vec{H}_2) \tag{47}$$

$$\vec{M}_s = -\hat{n} \times (\vec{E}_1 - \vec{E}_2) \tag{48}$$

Now, slightly above the surface of the ground plane there exists no electric field. Therefore we may conclude that only electric currents are present. In the slot however for the time being, we have both magnetic and electric currents. We are only interessted

in the field in Region 1 so, this means that we can choose the field in Region 2 arbitrarily. Let us choose this field to be zero. Then it does not matter what material we have in Region 2. That is, we can without hessitation place a large ground plane just behind the slot (Figure 11).

Now on the other hand, the electric current that was present on the original ground plane (and in the slot) in which the slot was mounted, cannot produce any radiation. This is beacause the image of the electric current is of the opposite sign and so the radiation from the two currents cancel out. This is only true if the two currents are located close to each other which they are in this case. So we are left with a single magnetic current above a large ground plane radiating into the dielectric sheet and free space (Figure 12). This ground plane may now be removed if the effect on the radiation is preserved by multiplying the magnetic current by a factor of 2 (Figure 13). The factor of 2 comes from the current image on the other side of the interface making the boundary conditions stiil satisfied. Note, that the field is only valid for Region 1. The field in Region 2 may be calculated by using the same method. It should also be noted that using this method the electric field is automatically made continuous in the aperture.

3.6.1 Slot radiating into a cavity or waveguide.

A slot that is radiating into a cavity or a waveguide can be treated in the same manner as a slot radiating into free space or a dielectric slab. The only difference is how we treat the current. Now, a magnetic current in the wall of a waveguide or cavity may also be treated by imaging techniques. Using this method we can transform the magnetic current in the closed region into another periodic current radiating into free space. Of course, we still have the third wall opposite to the slot to take care of. Howver, as explaned earlier in the previous chapters, the third wall can be treated by equivalent transmission lines in the spectral domain by applying the two-dimensional Fourier transform to Maxwell's equations.

The Green's function for the closed region has been discussed in a previous section and we therfor do not rephrase this. It should only be noted that the spectral domain technique, splitting into TE- and TM equivalent transmission line circuits, is a powerful method that can be used to solve many problems in planar structures. This also includes scattering from dichroic surfaces which implies the introduction of Floquet modes. Using the spectral domain technique and a periodic magnetic current will automatically give the electric and magnetic fields in terms of Floquet modes.

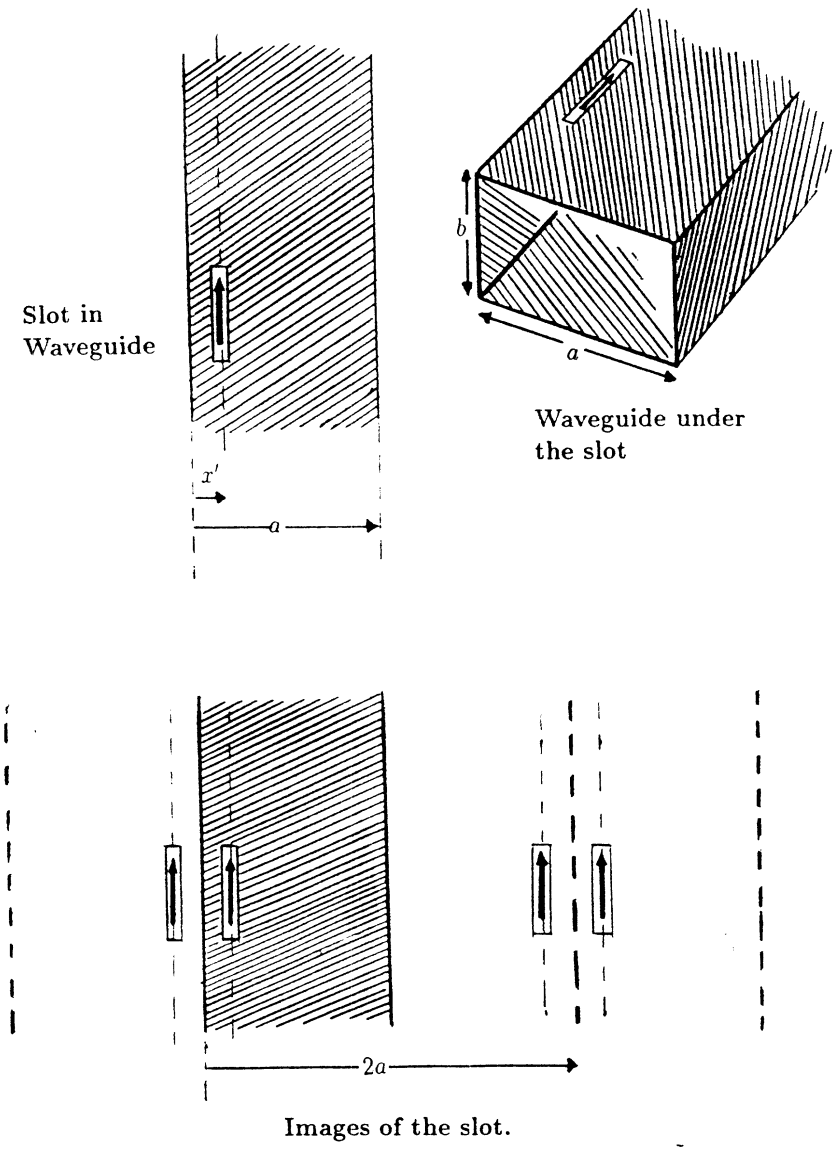

Figure 7: The magnetic current in the broad face of a rectangular waveguide. The walls can be removed if the original current is replaced by a periodic current as indicated.

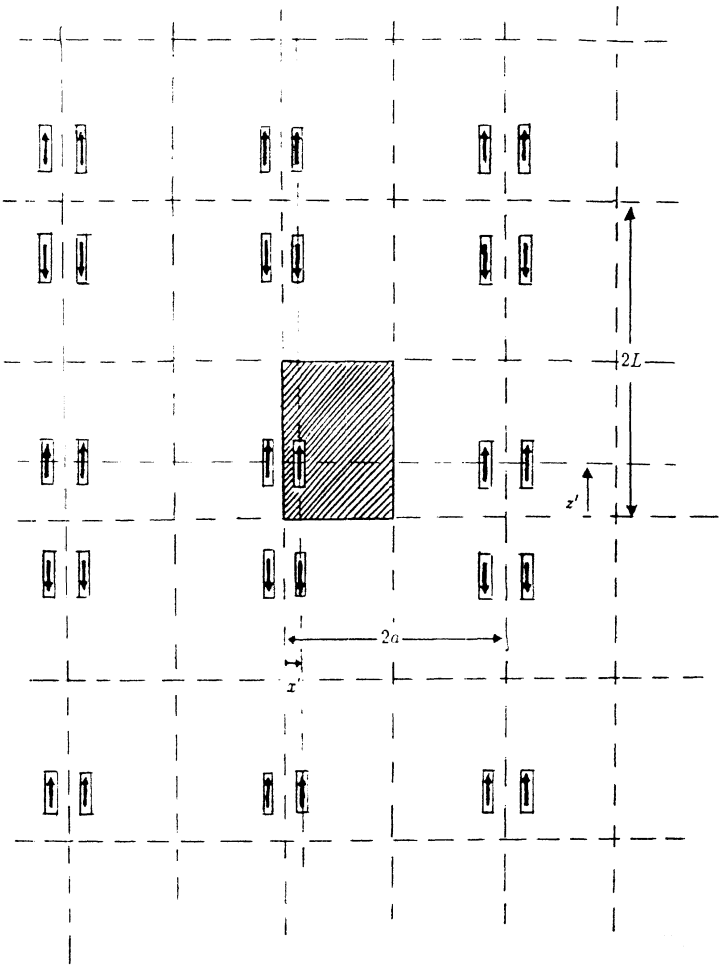

Figure 8: The magnetic current can be replaced by a periodic current in two dimensions. The current changes sign in the z-direction while it keeps the sign in the x-direction. This gives rise to cosine and sine factors in the field expressions.

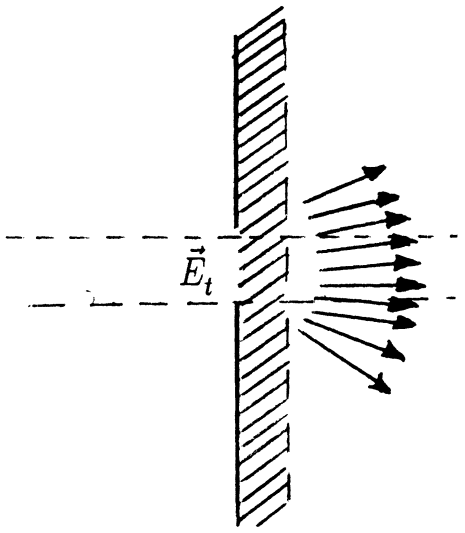

Figure 9: Slot radiating into a dielectric layer and into free space.

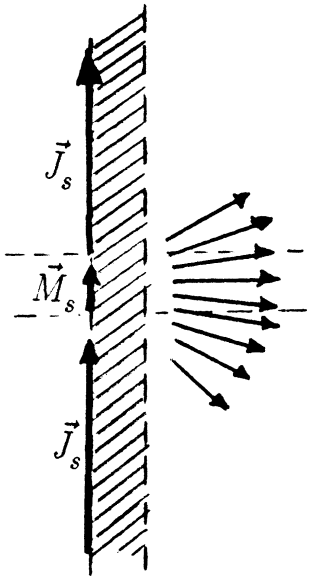

Figure 10: Equivalent electric and magnetic currents giving the same field as in the original situation depicted in Figure 9. The magnetic current on the original ground plane is zero since the tangential electric field is zero there.

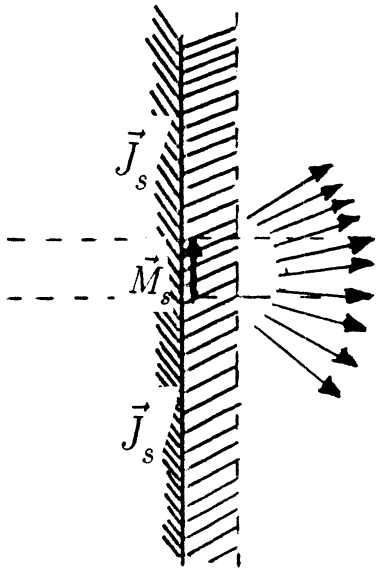

Figure 11: The currents in Region 2 are arbitrarily chosen. Therfor we can choose to replace the material in Region 2 by metal just behind the slot aperture.

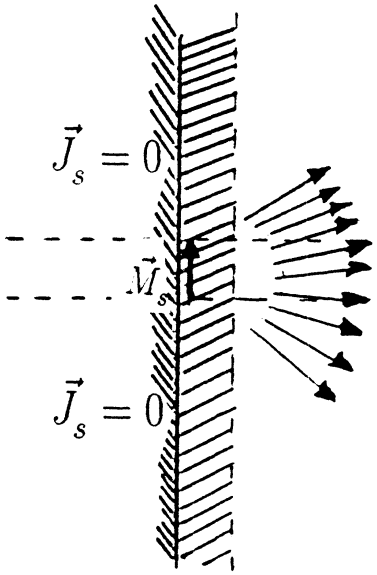

Figure 12: The electric current at the metal is short-circuited by the metal. Only the magnetic current remains.

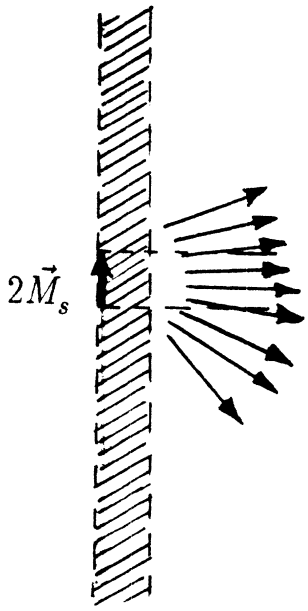

Figure 13: The ground plane is taken away and the magnetic current is multiplied by a factor of 2 to compensate. The radiated field from the magnetic current only yields Region 1.

4 The far-field radiation from a planar magnetic or electric current.

The far field from a planar source can be expressed in a very compact form by using only the inverse Fourier transform of the near field [9]. Of course, the far field can be computed by first calculating the electric and magnetic vector potentials which then gives the far field by dropping the higher order terms when performing the vector curl operation. However, the field from a planar source in a planar stratified dielectric medium is expressed more easily by means of two-dimensional Fourier transforms. Assume that the magnetic or electric current source is placed in the xz-plane and that the y-axis is perpendicular to the antenna structure Figure 14. The field from this structure can then be found by using the Fourier-type expressions as used in Eqs. (10) and (11) in Section 3.1. We rephrase these expressions but with the magnetic filed H replaced by the electric filed E for convenience:

$$E_z(x,y,z) = \int_{-\infty}^{+\infty}\int_{-\infty}^{+\infty} \hat{E}_z(k_x,y,k_z)\, e^{-j(k_x x + k_z z)}\, dk_x dk_z \tag{49}$$

$$E_x(x,y,z) = \int_{-\infty}^{+\infty}\int_{-\infty}^{+\infty} \hat{E}_x(k_x,y,k_z)\, e^{-j(k_x x + k_z z)}\, dk_x dk_z \tag{50}$$

Since this field is already expressed by a Fourier transform, basically the result will be just the integrand with k_x and k_z replaced by the directions cosine and sine. That is:

$$k_x \rightarrow k_0 \sin\theta\cos\phi \tag{51}$$

$$k_z \rightarrow k_0 \cos\theta \tag{52}$$

Now, the radiated field $\hat{E}_z(k_x,y,k_z)$ and $\tilde{E}_z(k_x,y,k_z)$ can directly be related to the field $\tilde{E}_z(k_x,0,k_z)$ and $\hat{E}_z(k_x,0,k_z)$ at the surface of the antenna, by:

$$\tilde{E}_z(k_x,y,k_z) = \hat{E}_z(k_x,0,k_z)\, e^{-jk_y y} \tag{53}$$

$$\tilde{E}_x(k_x, y, k_z) = \tilde{E}_x(k_x, 0, k_z)\, e^{-jk_y y} \tag{54}$$

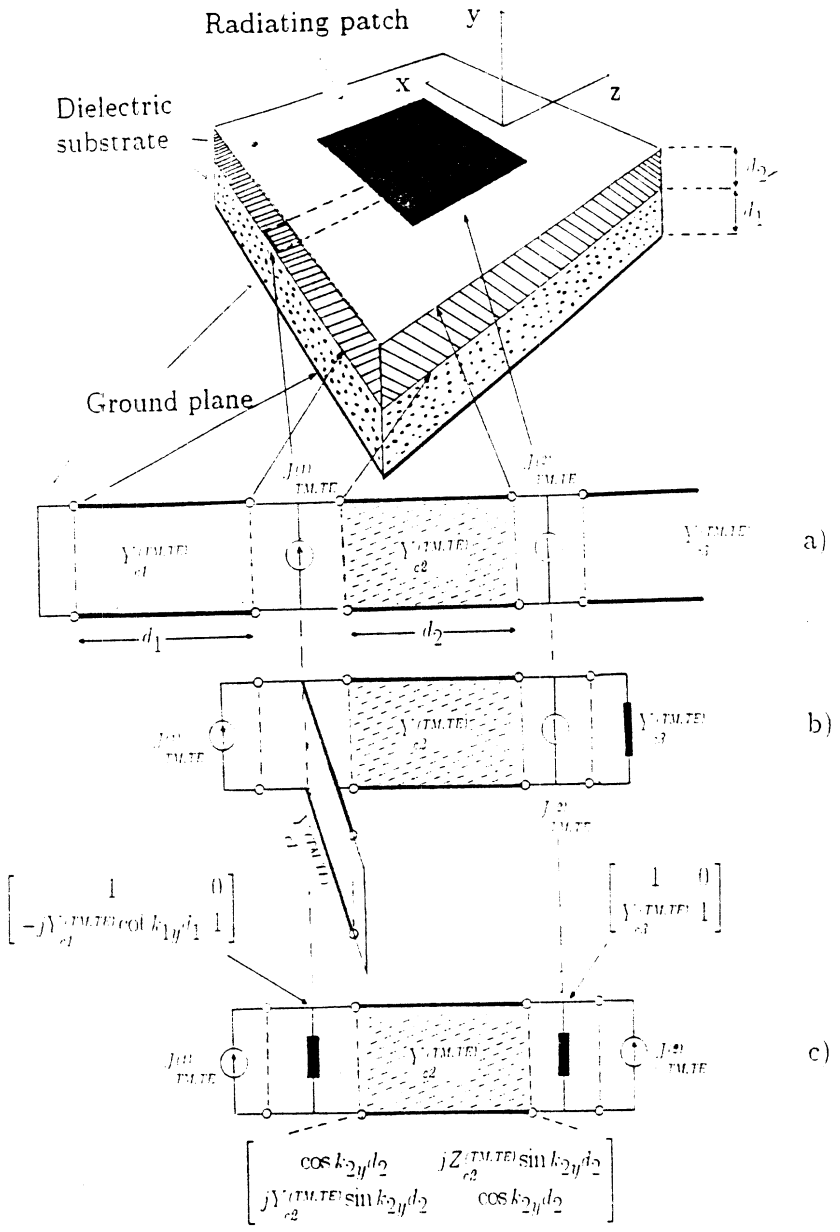

Figure 14: A general microstrip patch antenna and its equivalent transmission line circuit in the spectral domain.

So, we have the following expressions for the radiated field instead:

$$E_z(x, y, z) = \int_{-\infty}^{+\infty}\int_{-\infty}^{+\infty} \tilde{E}_z(k_x, 0, k_z)\, e^{-j(k_x x + k_y y + k_z z)}\, dk_x dk_z \tag{55}$$

$$E_x(x,y,z) = \int_{-\infty}^{+\infty}\int_{-\infty}^{+\infty} \tilde{E}_x(k_x,0,k_z)\, e^{-j(k_x x + k_y y + k_z z)}\, dk_x dk_z \tag{56}$$

Rhodes [9] gives an asymptotic expression for this kind of integral as $r = \sqrt{x^2+y^2+z^2} \to \infty$. By use of this expression, we directly obtain the rectangular components in the far field as:

$$\lim_{r\to\infty} E_z(r,\theta,\phi) \sim \cos\Psi\, \tilde{E}_z(k_x,0,k_z) \tag{57}$$

$$\lim_{r\to\infty} E_x(r,\theta,\phi) \sim \cos\Psi\, \tilde{E}_x(k_x,0,k_z) \tag{58}$$

where:

$$k_x = k_0 \sin\theta\cos\phi \tag{59}$$

$$k_z = k_0 \cos\theta \tag{60}$$

$$\cos\Psi = \hat{y}\,\hat{r} = \sin\theta\sin\phi \tag{61}$$

It now remains to calculate the spherical components $E_\theta(r,\theta,\phi)$ and $E_\phi(r,\theta,\phi)$ in the far field. We leave this to the reader as an exercise or to consult other literature. We summarize the expressions for the far field radiated from a planar structure in the following table:

$$E_\phi(r,\theta,\phi) \sim -\sin\theta\tilde{E}_x(k_x,0,k_z) - \cos\phi\cos\theta\tilde{E}_z(k_x,0,k_z)$$

$$E_\theta(r,\theta,\phi) \sim -\sin\phi\,\tilde{E}_z(k_x,0,k_z)$$

$$\tilde{E}_x(k_x,0,k_z) = \frac{1}{\sqrt{k_x^2+k_z^2}}\left[-V_{TE}(k_x,0,k_z)k_z + V_{TM}(k_x,0,k_z)k_x\right]$$

$$\tilde{E}_z(k_x,0,k_z) = \frac{1}{\sqrt{k_x^2+k_z^2}}\left[V_{TE}(k_x,0,k_z)k_x + V_{TM}(k_x,0,k_z)k_z\right]$$

where:

$$k_x = k_0 \sin\theta \cos\phi$$

$$k_z = k_0 \cos\theta$$

5 The moment method applied to slot antennas.

The method of moments has successfully been applied to solve many problems in electromagnetics and antenna engineering. It provides an efficient tool for computation of antenna characteristics like radar cross section, radiation impedance and input impedance. Normally, these problems call for the solution of complicated coupled integral equations accounting for current interaction between different parts of the antenna. Only in the most trivial cases it is possible to obtain an explicit solution by making simplifying assumptions and comparisons with canonical integral equations. By using the method of moments, however, the problem can be transformed into a linear matrix equation instead. The unknown variables in this matrix equation are then used as the amplitudes of known basis functions defining the unknown current distribution. It is in the end therefore possible to obtain a solution by using basic mathematical tools familiar to every engineer. This fact makes the method applicable and attractive to a wide class of electromagnetic problems [8].

5.1 The general formulation

The basic idea of the moment method is to transform an integral equation for the unknown magnetic or electric currents into a set of linear equations. In this way, the currents can be obtained directly from the unknown vector of this matrix equation by basically performing a matrix inversion. The integral equation can either be formulated by enforcing zero tangential electric field on the surface of conducting bodies or by enforcing continuity of the magnetic field across apertures. The former equation is called the electric field integral equation (EFIE) while the latter is called the magnetic field integral equation (MFIE). Sometimes you can also formulate a mixed integral equation. Since the antenna in this report consists of slots cut in an infinite ground plane, we are however only concerned with the solution of the MFIE in this report. Using the method of moments, the unknown currents are expanded in a finite series of known basis functions with unknown coefficients. This expansion is then inserted into the integral equation and, finally the matrix equation is obtained by applying an inner product with respect to a set of testing functions. In this report we use the same set of testing functions as we use for the basis functions. This is called the Galerkin method.

Let the tangential external and internal magnetic field due to the incident and the induced currents be denoted by $\vec{H}_t^{inc}(x,z)$ and $\vec{H}_t^{ext}(x,z)$ and $\vec{H}_t^{ext}(x,z)$ respectively. The coefficients of these current modes are then the unknown quantities which have to be solved in order to satisfy the integral equation. The procedure to find the coefficients is outlined as follows. We start by formulating the integral equation (MFIE) forcing the total tangential magnetic field in the slots to be continuous. The MFIE is written as:

$$\vec{H}_t^{ext}(x,z) + \vec{H}_t^{inc}(x,z) = \vec{H}_t^{int}(x,z) \qquad \text{(Integral equation)} \qquad (62)$$

Further, let $\mathcal{L}_{ext}$, $\mathcal{L}_{int}$ denote linear operators acting on the expressions for the electric field in the slot apertures and let $\vec{H}_t^{inc}(x,z)$ be the impressed tangential magnetic field in the slot. General expressions for these operators are also derived in this report. By use of these operators, the above integral equation can then be expressed as:

$$\mathcal{L}_{ext}\left[\vec{E}_t(x,z)\right] + \vec{H}_t^{inc}(x,z) = \mathcal{L}_{int}\left[\vec{E}_t(x,z)\right] \qquad (63)$$

The next step in the method of moments is to approximate the induced field in the slot by a finite series expansion with coefficients E_n. The induced field will in general have two orthogonal components, so using vector notation we write the expansion as:

$$\vec{E}_t(x,z) = \sum_{n=1}^{N} E_n \vec{E}_{t,n}(x,z) \qquad \text{(Induced field expansion.)} \qquad (64)$$

This expansion is then inserted into the integral equation in Eq. (63). We obtain a modified integral equation, as (modified since it is now only approximate):

$$\mathcal{L}_{ext}\left[\sum_{n=1}^{N} E_n \vec{E}_{t,n}(x,z)\right] + \vec{H}_t^{inc}(x,z) = \mathcal{L}_{int}\left[\sum_{n=1}^{N} E_n \vec{E}_{t,n}(x,z)\right] \qquad (65)$$

Using the linearity property of the operators $\mathcal{L}_{ext,int}$ we can let them act on each term of the expansion instead of the total field. It is further noticed, that the operators $\mathcal{L}_{ext,int}$ actually depend on the type of field mode as well. That is, we have to use different Green's functions depending on where the currents are located. We therefore formally write the operator $\mathcal{L}$ with an additional index n as $\mathcal{L}_n$. This gives:

$$\sum_{n=1}^{N} I_n \mathcal{L}_{ext,n}\left[\vec{E}_{t,n}(x,z)\right] + \vec{H}_t^{inc}(x,z) = \sum_{n=1}^{N} I_n \mathcal{L}_{int,n}\left[\vec{E}_{t,n}(x,z)\right] \qquad (66)$$

This equation does only approximately hold since we have introduced an approximation to the induced current in Eq. (64). The error can however be minimized by applying a set of testing functions $\vec{W}_m(x,z)$ $(m = 1 \cdots N)$ according to the method of moments [8]. We then get the following set of equations for $m = 1, 2 \cdots N$:

$$\sum_{n=1}^{N} I_n <\mathcal{L}_{ext,n}\left[\vec{E}_{t,n}(x,z)\right] \, . \, \vec{W}_m(x,z)> \, + \, <\vec{H}_t^{inc}(x,z) \, , \, \vec{W}_m(x,z)> \, =$$

$$= \sum_{n=1}^{N} I_n <\mathcal{L}_{int,n}\left[\vec{E}_{t,n}(x,z)\right] \, . \, \vec{W}_m(x,z)> \tag{67}$$

where the inner product is defined as the integral over the some surface S, as:

$$<g,h> \, = \int\int g(x,z)h^*(x,z) \, dx \, dz \tag{68}$$

The matrix equation in Eq. (67) can finally be written in a more compact form, as:

$$\sum_{n=1}^{N} I_n \cdot A_{mn} \, = \, B_m \qquad\qquad m = 1, 2, 3 \cdots N \tag{69}$$

where:

$$A_{mn} \, = \, <\mathcal{L}_n\left[\vec{J}_n^{ind}(x,z)\right] \, . \, \vec{W}_m(x,z) > \tag{70}$$

$$B_m \, = \, - <\mathcal{F}\left[\vec{J}^{inc}(x,z)\right] \, , \, \vec{W}_m(x,z) > \tag{71}$$

It should be noticed that the magnetic field in the slot apertures in general has two components. So the testing function $\vec{W}_m(x,z)$ is in general also a two-component vector. The matrix elements A_{mn} and the vector elements B_m are however only scalar quantities

6 Computed current on different parts of the antenna.

6.1 Two slot lines forming a microshield line: with and without coupling included.

In order to check the output of the program it is always wise to check different sub-parts first. That is, to begin with we do not need to include both the internal (inside the waveguide) and external (outside the waveguide) parts of the problem. If we first only study the external part as if the antenna structure was radiating into free space then we will get a fairly good idea of the behavior of the antenna. The internal part can then be added afterwards to check the influence of the cut-off waveguide. Further, we want to go step by step by adding more and more parts to the antenna. That is we start with the microshield line alone, and then we add a dipole at the end of the feed line, and so on until the whole antenna is tested.

As a first check of the computer program we can check if the current in the two slots forming the feed line is correct. This current should form a standing wave with peaks separated by one half of a wavelength. Also, the peaks and minima should have the same amplitude. Now we may excite the two slots in any location we want. However, we want the location points to be far away from the antenna that we are going to feed. Therefore, we place our excitation point at the other end of the feed line. We choose to place it at the 10:th rooftop-function and we make this choice for both the slots. Also, the excitation is 'odd' meaning that the upper line is excited by +1 and the lower line is excited by -1. This will give a pattern null in the H-plane cut of the feed line diagram. At the same time there will be an in-phase radiation from the two radiating slot dipoles which are going to be included later on. The length of the slots are chosen in order to obtain a maximum field strength at the end of the feed line when the antenna is working at resonance frequency. Figure 15 shows the magnetic current when no coupling between the slots is included and Figure 16 shows the influence when the coupling is included.

The currents are computed using only the free space part of the admittance matrix. The internal part is added to the external later in this report. Also, for the moment we only look at the operating frequency chosen as 25.53 GHz.

Data:

Number of rooftop functions in the slot.	59
Size of each cell (mm)	0.25
Distance 2w between the slot edges (mm)	0.5
Slot width (mm)	0.25
Frequency (GHz)	25.53

We see from Figure 15 and 16 that the current forms a nice standing wave pattern with peaks at regular distances. The distance between the peaks is close to one half wavelength in free space. The only difference when taking the coupling between the two slots into account is that the amplitude is somewhat affected. One might conclude that the radiation in the coupled case is less. This is reasonable and it is concluded that this part of the program is working as expected. The end-reactance of this short-circuited feed line can easily be calculated by the standing wave ratio and the distance of the first maxima to the end point (see Appendix A). It is also clearly seen where the excitation is placed. The currents have a peak at this position.

6.2 Microshield line feeding a slot dipole radiating into free space.

The next step is to include a dipole at the end of the microshield line. The dipole is formed by the same basis functions as were used in the preceeding subsection. In order to be compatible with the loop antenna that is going to be tested further on in this report we choose the dipole length to be about 0.36λ at 25.53 GHz. Figure 17 shows the electric field in the upper part of the microshield line. The current has a maximum at the center point of the dipole as was pressumed in the foregoing section. This looks in proper order. It is also seen from Figure 18 that the electric field distribution in the dipole is symmetrical and has a maximum at the center as it should.

6.3 A loop antenna fed by the microshield feed line.

As earlier mentioned, we want to feed a radiating antenna with the new microshield line. We have already studied the influence of adding a dipole antenna but we also want to see what happens if we feed other types of radiating structures. A simple antenna that can be fed using the microshield transmission line is the loop antenna that is depicted in Figure 19. If the feed line is excited in the odd mode then only parts 1 and 2 will radiate in phase. All the other slots will radiate out of phase to each other.

Number of basis functions on X_1	N_{X_1}	59
-"- X_2	N_{X_2}	8
-"- X_3	N_{X_3}	8
-"- X_4	N_{X_4}	59
-"- Y_1	N_{Y_1}	7
-"- Y_2	N_{Y_2}	17
-"- Y_3	N_{Y_3}	7
Dimension of one quadratic cell	D_c	0.25 mm

The length of the loop is adjusted so that the length L is approximately $\lambda/2$ at the design frequency. Further, the lines (1) and (2) that are assumed to radiate in phase are kept as long as possible in order to increase radiation.

Figure 20 and Figure 21 shows the magnitude of the total current on the upper feed line x_1 and the lower feed line x_4 respectively. From the maximum and minimum we can calculate the standing wave ratio (S=5.2) and from that we get the input reflection coefficient $\Gamma = 0.67$. This reflection coefficient is in general a litle too high for antenna applications but we can always match the antenna by for eaxmple a quarter wavelength transformer or a similar structure. The field strength in the left most dipole (1) and the right most dipole (2) is plotted in Figure 22 and Figure 23 respectively. The field is in phase and the field strength is approximately the same too.

6.4 Adding the internal part of the damittance matrix to the loop antenna.

Now we want to add the internal part of the admittance matrix. The elements only have non-zero values in the imaginary parts. Moreover the imaginary parts are approximativly the same as in the free space case if the waveguide walls are far apart from the slot sections. Therefore, we may in advance suspect that the currents should have the same form exept in regions close to the waveguide wall. This is verified by looking at the plotted electric field strength in parts (3) and (4) of the antenna. The currents on the (3) and (4) parts do not cross the zero level at the same place as when the antenna is radiating into free space (Figure 24 and Figure 25). The influence of the waveguide wall is making the effective propagation factor in the number (3) and (4) slot different from other parts of the antenna. This basically affects the oprating frequency of the antenna. That is, the two in-phase radiating slots are slightly out of phase to each other by a few degrees ($5° - 10°$). The field strength in the dipoles and the feed line are plotted in Figure 26 to Figure 28.

6.5 Quarter wavelength transformer.

In order to better match the loop antenna to the microshield line a quarter wavelength transformer was tested Figure 29. Such a transformer consists of a quarter wavelength section of a transmission line with an impedance Z_c that satisfies the following condition.

$$Z_c^2 = Z_1 Z_2 \tag{72}$$

where Z_1 and Z_2 are the two impedances to be matched to each other. Now, this implies that Z_1 and Z_2 should be real if the characteristic impedance Z_c of the transformer is real. Having an input impedance of the antenna that is in general not real we cannot get a pure impedance match. However, we always can make the input reflection coefficient lower. A simple transformer is easily constructed by adding another row of rooftop functions above the original feed lines. If we let this new line be a quarter wavelength shorter then we will obtain the desired transformer. This is tested below.

In this test we do not include every coupling coefficient in the structure. This would be a too elaborate thing to do. We meerly want to see the reaction on the standing wave ratio as we introduce the transformer. That is, only the coupling between the nearest lines is included. Figure 30 shows the field strength on the feed line for different lengths of the transformer section. The results are divided into two figures. Figure 31 shows the rest of the curves. It is seen that one can obtain a better match with this transformer section. However, it would probably be a better choice to make a matching network using a tuning capacitive stub at a certain distance from the antenna. Such stubs can be made separately on the microshield line without large coupling to the radiating part of the antenna.

Number of basis functions on X_1	N_{X_1}	59
-"- X_2	N_{X_2}	8
-"- X_3	N_{X_3}	8
-"- X_4	N_{X_4}	59
-"- Y_1	N_{Y_1}	7
-"- Y_2	N_{Y_2}	17
-"- Y_3	N_{Y_3}	7
-"- X_5	N_{X_5}	41-47
-"- X_6	N_{X_5}	41-47
Dimension of one quadratic cell	D_c	0.25 mm

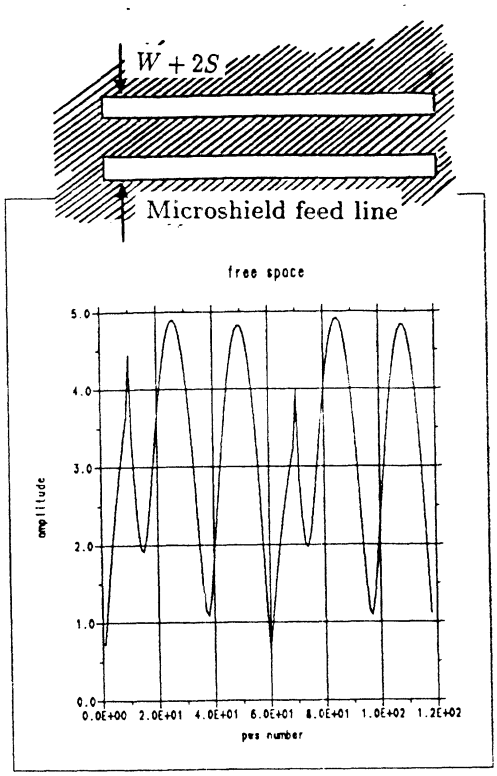

Figure 15: Electric field strength (magnetic current) in the microshield feed line when the coupling between the slots is not included. The geometrical and electrical data are given in Table 6.1. Modes corresponding to the upper line are numbered 1...59 and those to the lower line are numbered 60-118.

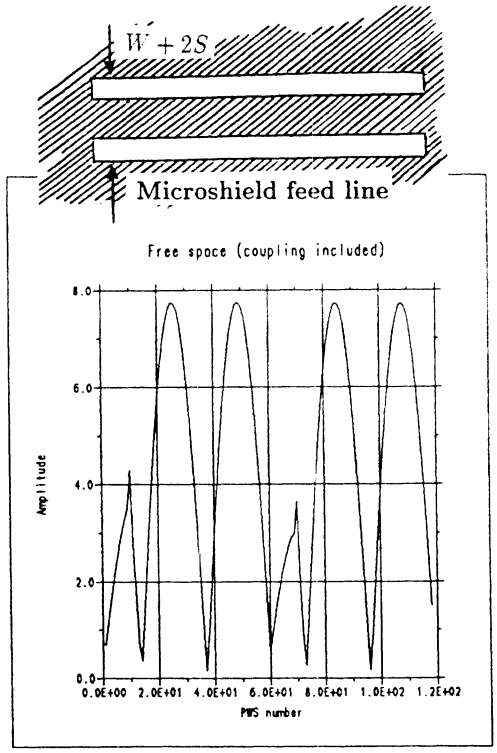

Figure 16: Electric field strength (magnetic current) in the microshield feed line when coupling between the slots is included. The geometrical and electrical data are given in Table 6.1. Modes corresponding to the upper line are numbered 1...59 and those to the lower line are numbered 60-118.

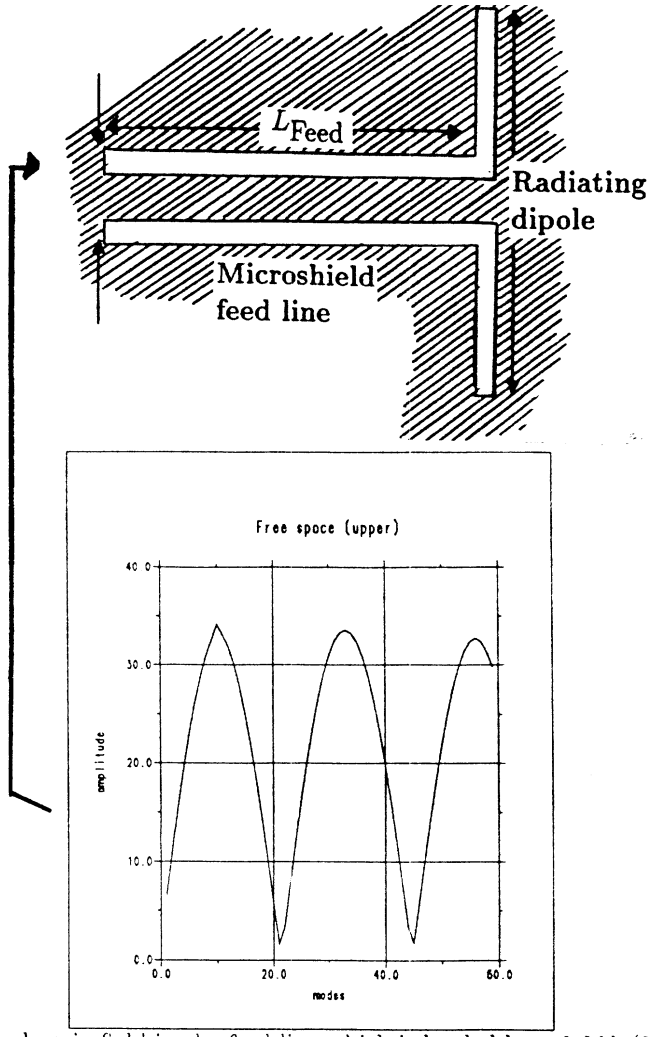

Figure 17: The electric field in the feed line which is loaded by a 0.36λ (25.53 GHz) slot dipole at the end. The geometrical and electrical data are listed in Table 6.1.

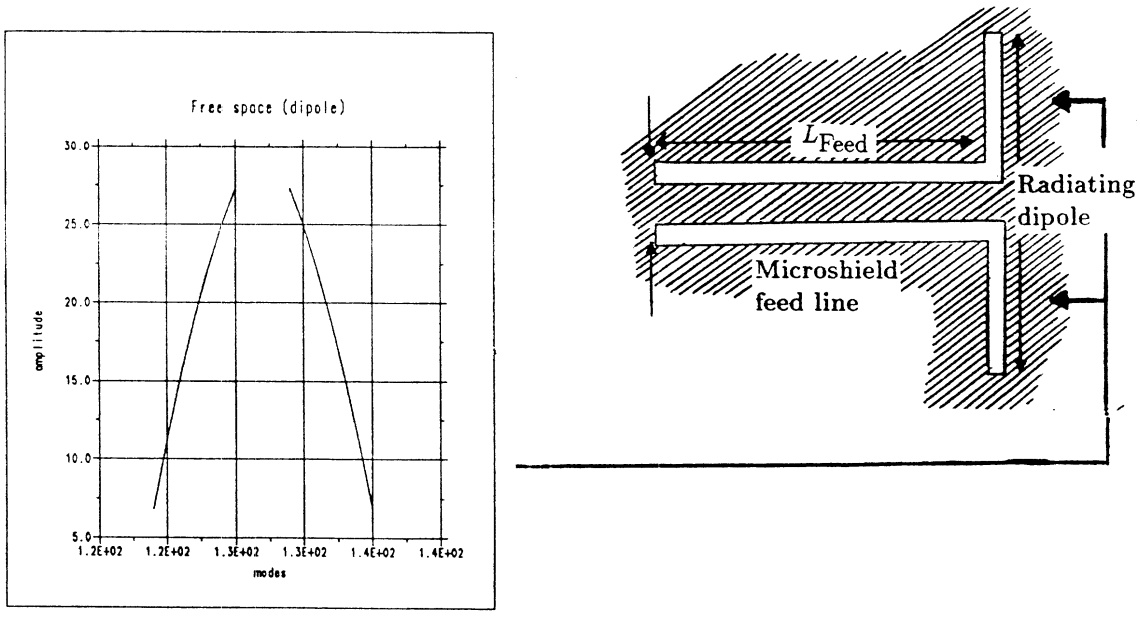

Figure 18: The electric field in the dipole which is fed by the feed line. The geometrical and electrical data are listed in Table 6.1.

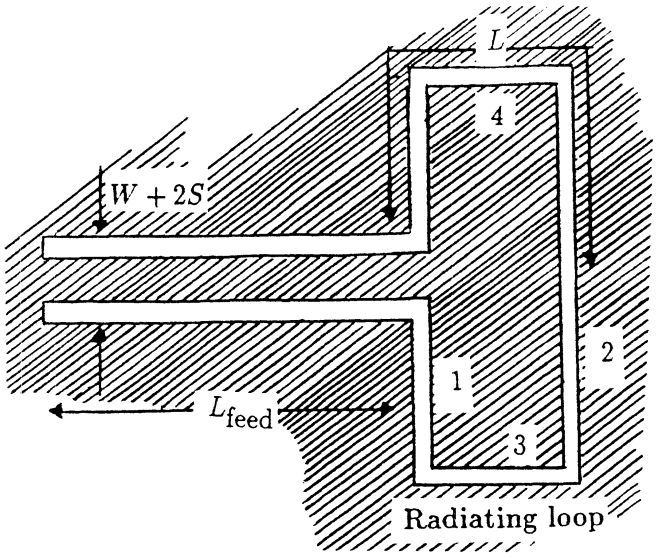

Figure 19: The loop antenna which is fed by the microshield line. In the same figure we have indicated the notation for the number of basis functions of various parts of the antenna.

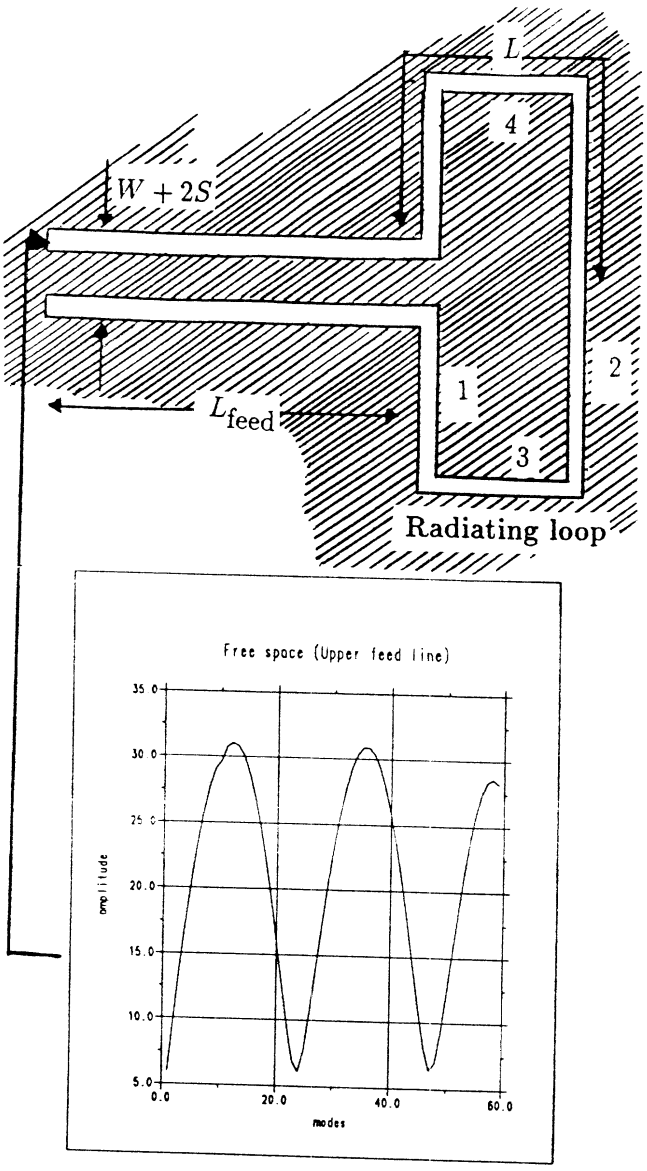

Figure 20: The electric field in the upper part of the microshield feed line. The field is a function of the mode numbers.

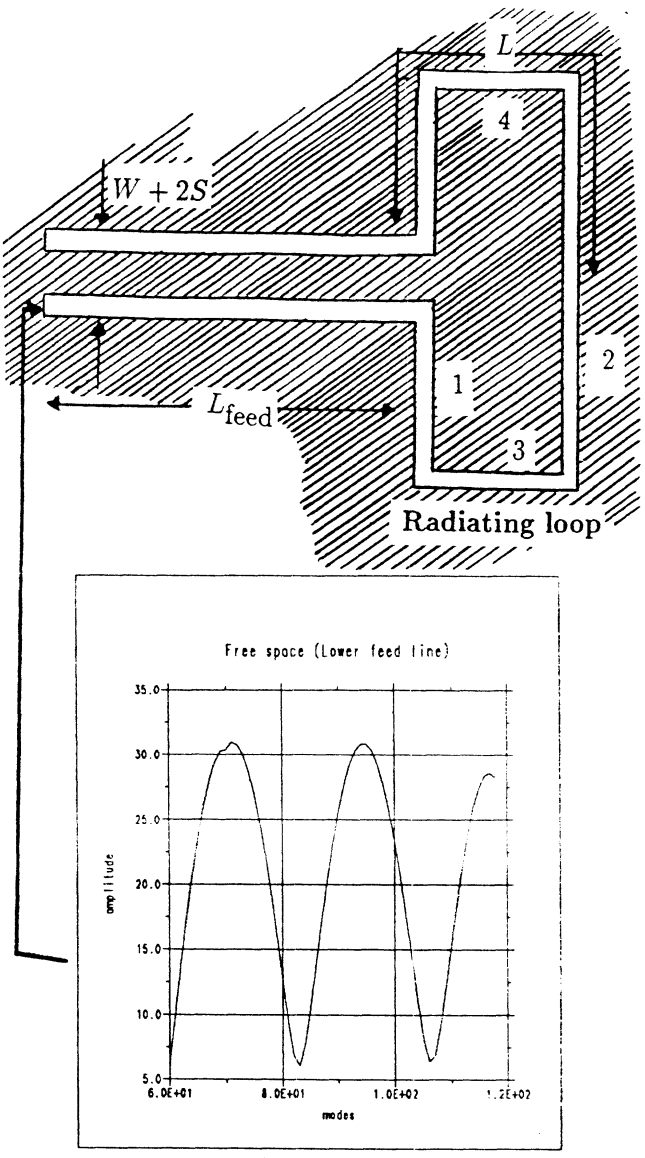

Figure 21: The electric field in the lower part of the microshield feed line. The field is a function of the mode numbers.

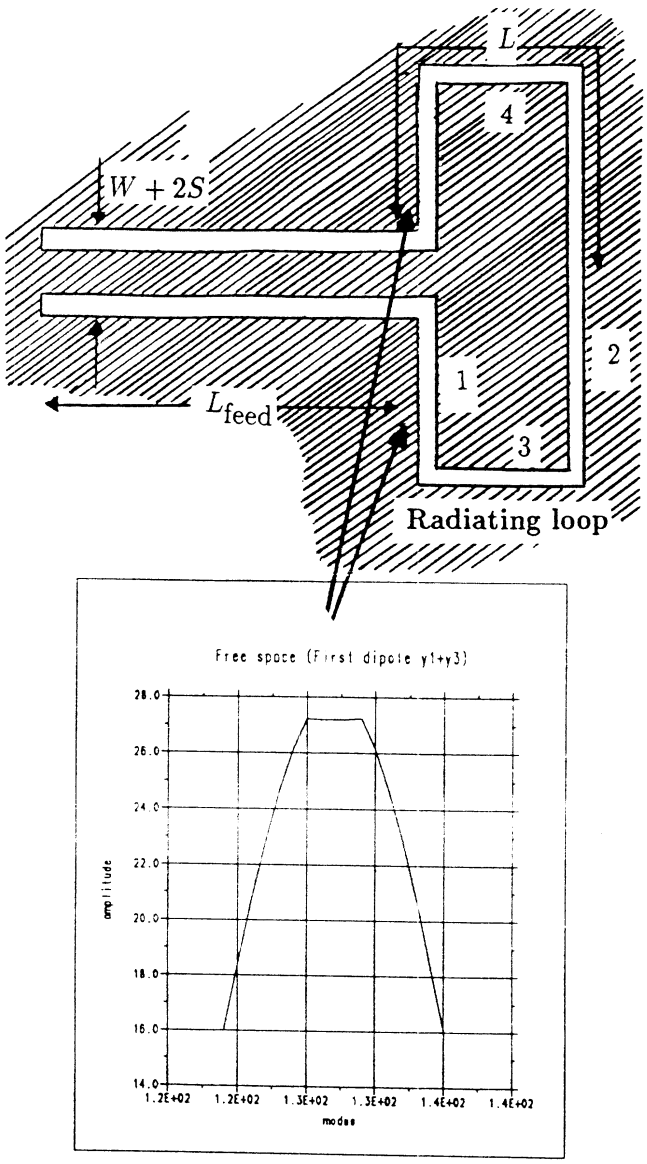

Figure 22: The electric field strength in the left dipole (1). The field is a function of the mode numbers.

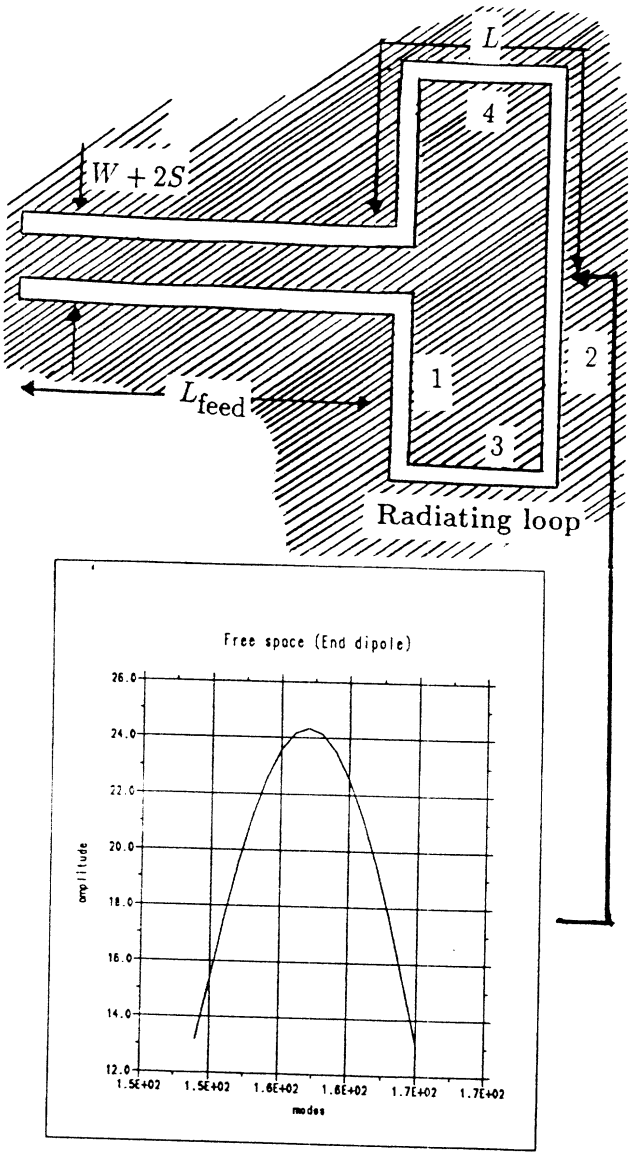

Figure 23: The electric field strength in the right dipole (2). The field is a function of the mode numbers.

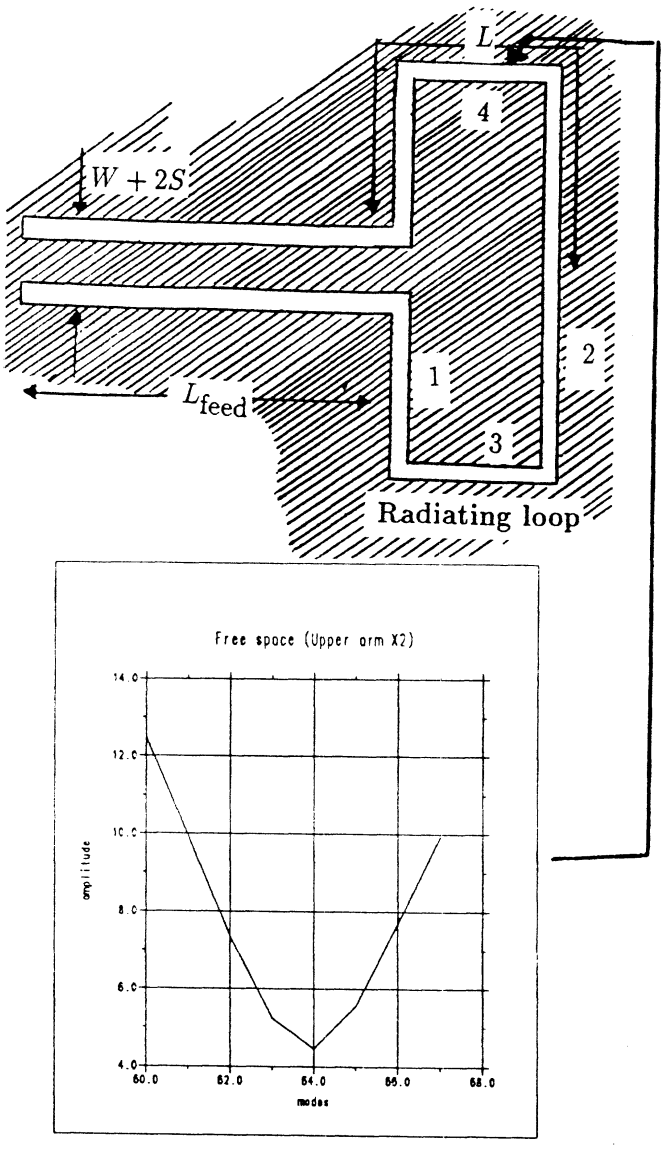

Figure 24: The field strength in part (3) and (4) of the loop antenna radiating into free space. No cavity is placed on the rear side of the loop antenna.

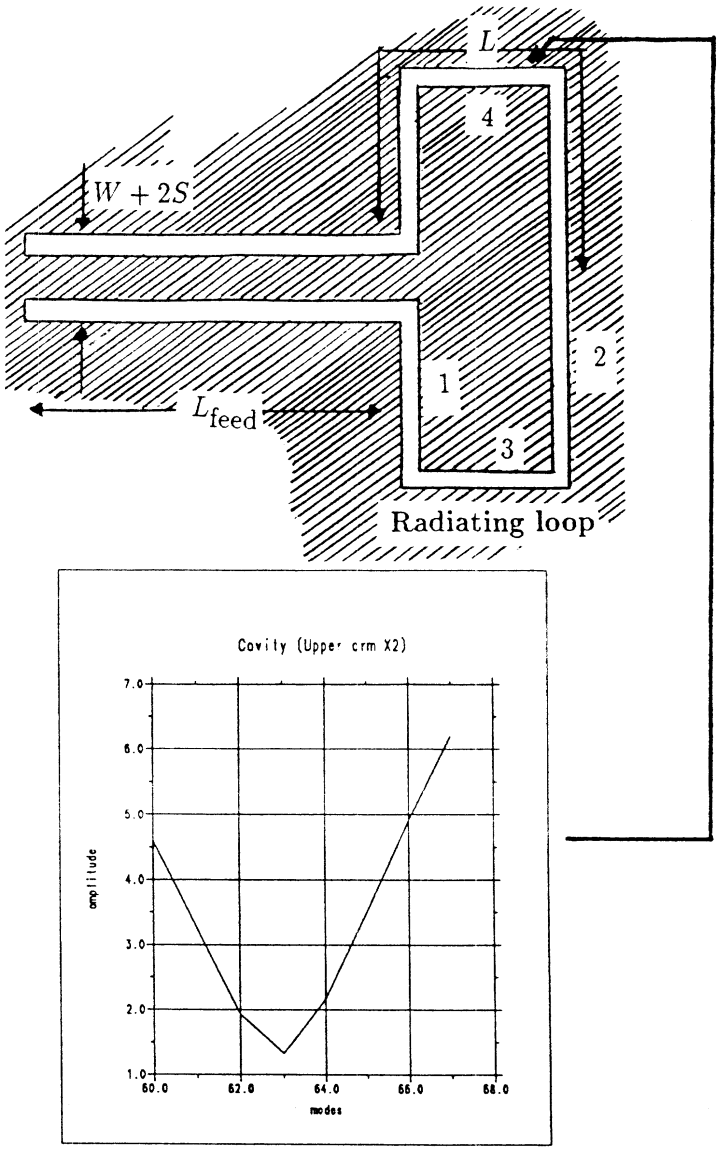

Figure 25: The field strength in part (3) and (4) of the loop antenna when the rear side is shielded by a cavity. The point where the field is minimum is moved slightly due to the waveguide walls near the feed line.

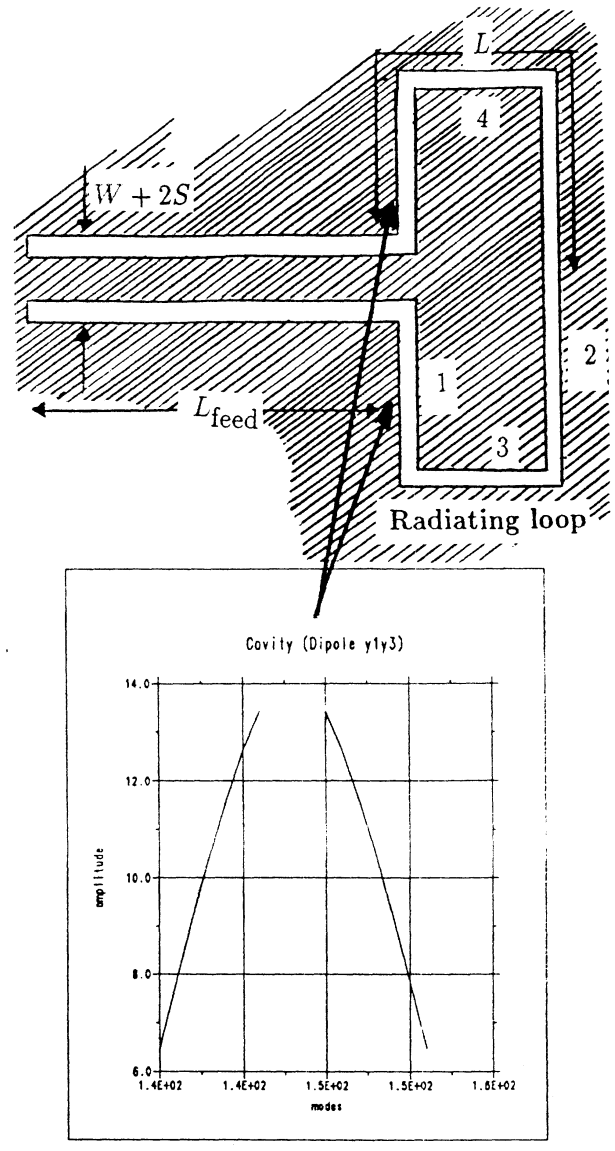

Figure 26: The field strength in the first (1) dipole of the loop antenna when shielded by a cavity on the rear side.

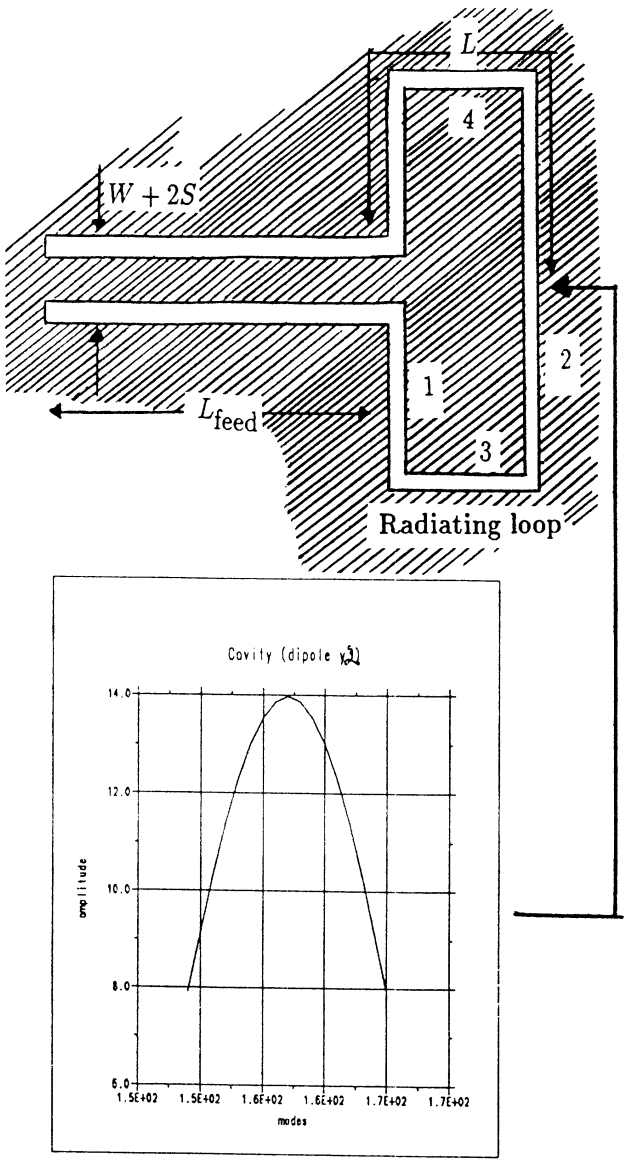

Figure 27: The field strength in the second (2) dipole of the loop antenna when shielded by a cavity on the rear side.

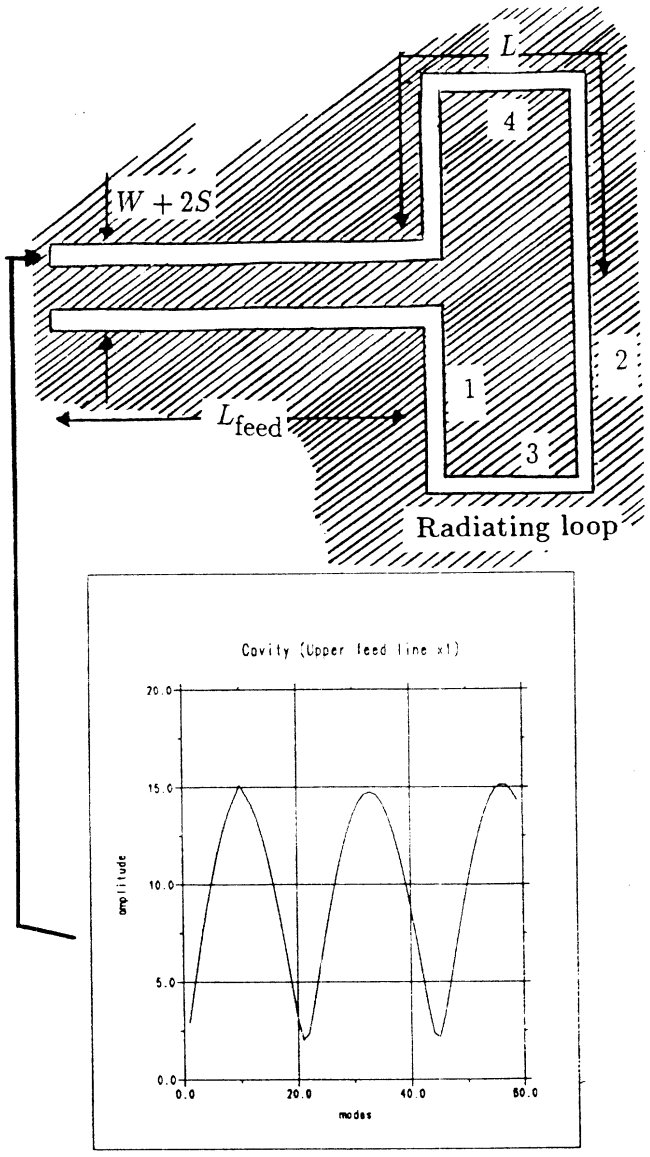

Figure 28: The field strength in the feed microshield line when feeding the loop antenna which is shielded by a cavity on the rear side.

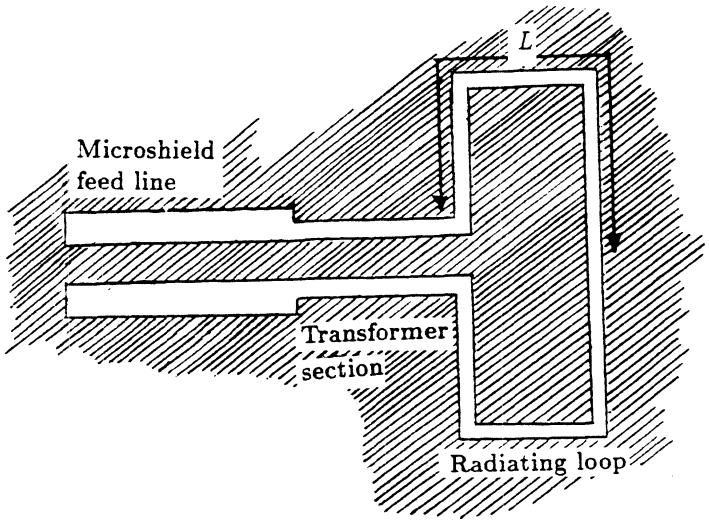

Figure 29: The loop antenna with a quarter wavelength impedance transformer. The length of the feed line to the left is varied between 41 and 47 number of basis functions. The number of basis functions on other parts are compiled in the tabel below.

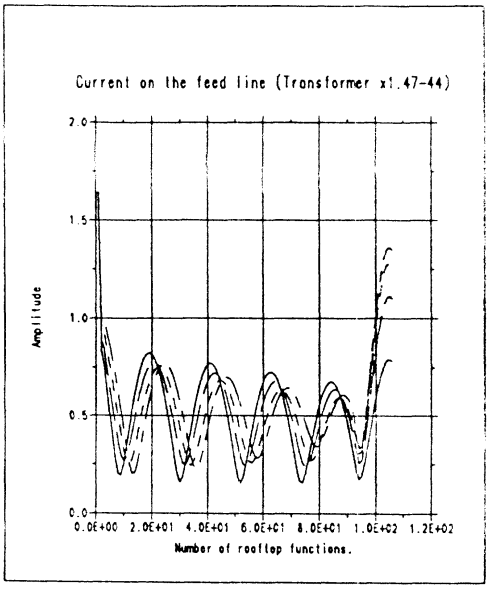

Figure 30: The electric field strength in the feed line for different lengths of the quarter wavelength transformer. The numbers 47-44 indicate the number of modes on the left most part of the feed line.

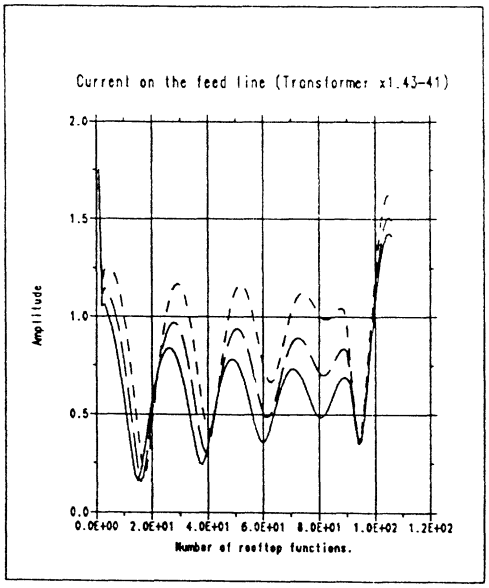

Figure 31: The electric field strength in the feed line for different lengths of the quarter wavelength transformer. The numbers 43-41 indicate the number of modes on the left most part of the feed line.

6.6 Input reflection coefficient for the loop antenna.

The reflection coefficient for the loop antenna as a function of frequency is shown in Figure 32. The different coefficients are shown between 22.98-27.45 GHz. The curve shows a minimum magnitude of reflection around the design frequency at 25.534 GHz. The curve is obtained by using a qubic spline fit of the real and imaginary parts of the input impedance. The spline curve shows a resonance loop around the design frequency 25.53 GHz. The input impedance can be matched to the microshield line by placing a tuned capacitive series stub at an appropriate distance from the antenna load plane.

Number of basis functions on X_1	N_{X_1}	59
-"- X_2	N_{X_2}	8
-"- X_3	N_{X_3}	8
-"- X_4	N_{X_4}	59
-"- Y_1	N_{Y_1}	7
-"- Y_2	N_{Y_2}	17
-"- Y_3	N_{Y_3}	7
Dimension of one quadratic cell	D_c	0.25 mm

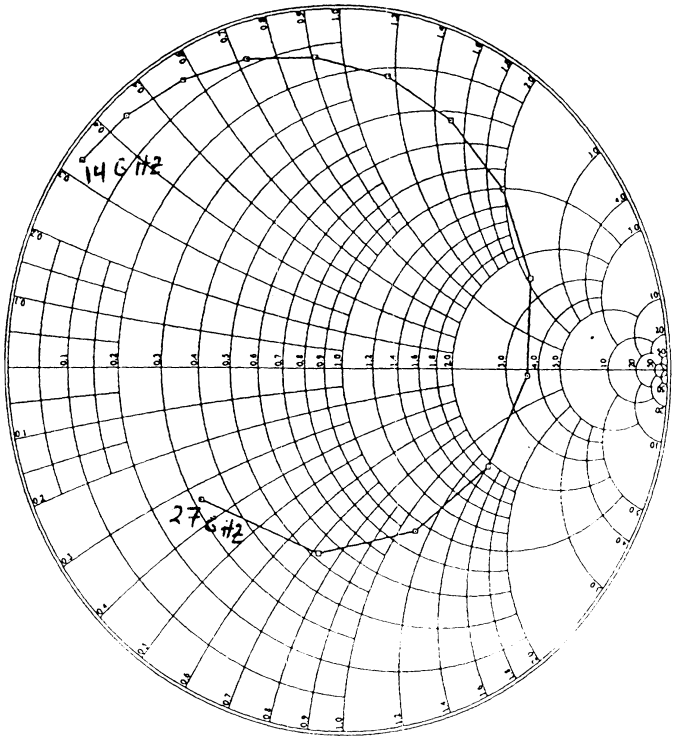

Figure 32: The predicted normalized impedance as a function of frequency for the microshield line-fed loop antenna. The reference plane is at the feed point of the loop. S=0.25 mm, W=0.5 mm, L is approximately $\lambda/2$ at 19 GHz.

6.7 The computed far-field from the loop antenna.

Having calculated the amplitudes of all the current elements by matrix inversion it is pretty straight forward to calculate the farfield radiation pattern. Every basis function in the antenna contributes to the far field by phase and magnitude and location in the array of basis functions. The equations for the far field are summarized in Section 4. Both the cross polarized and the co-polar field may be calculated by this method. These two orthogonal components are calculated separately since only one direction of the current causes radiation in a specified direction.

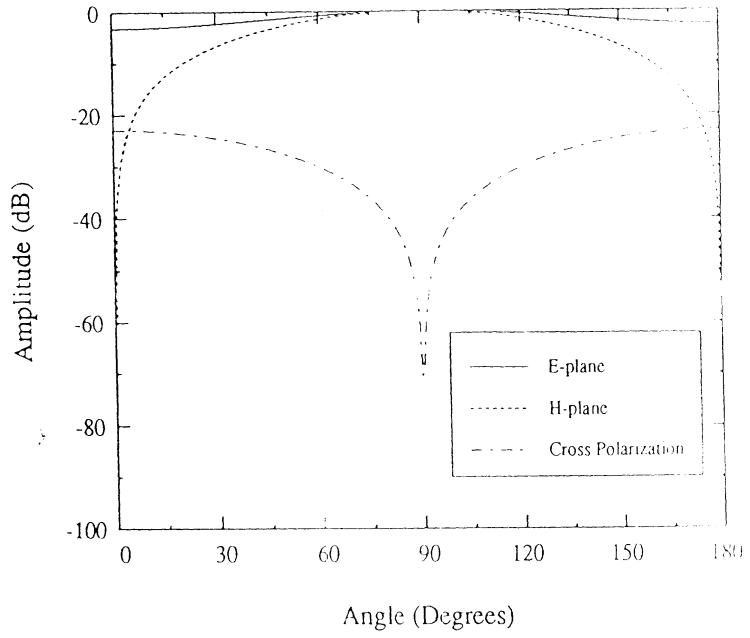

Figure 33: The predicted radiation pattern at the design frequency (19 GHz) for the loop antenna.

In Figure 33 It is seen that the E-plane cut is relativly flat while the H-plane cut is somewhat broader. As was expected, the cross-polar radiation is zero at broadside but increases as the observation angle increases. The cross-polar level might be expected to be lower than it actually is. The higher level is due to spurious radiation from the two arms denoted (3) and (4). Another configuration of the radiator might give a lower cross-polar radiation.

7 Conclusions

The microshield line is a suitable feed for antennas at frequencies in the sub-mm frequency range where radiation loss and ohmic losses might be a serious problem. The effective wavelength in the microshield structure is close to the free space wavelength which makes it easy to design an antenna for a specific frequency. Another advantage is that the size of the antenna is larger than when using dielectric substrates which simplifies the design at higher frequencies. Moreover, matching networks can be made using the same structure and be designed separately without including the radiating antenna. The low coupling in these kind of structures makes this possible. The relatively high cross-polar radiation level from the loop antenna at wide angles might be a problem. However, this radiation is due to the electric field in the out-of-phase parts of the loop antenna. Another design of the antenna is likely to reduce the cross-polar radiation level. It is concluded that the new monolithic microshield loop antenna can be used as a good low loss radiator at sub-mm frequency range.

References

[1] List of reports 1950-1985. Radiation Laboratory, Department of Electrical Engineering and computer Science, College of Engineering the University of Michigan Ann Arbor, Michigan

[2] N.I. Dib, W.P. Haropocus Jr., P.B. Katehi, C.C. Ling, and G.M.Rebeiz, "Study of a novel planar transmission line", NASA Center for Space Terahertz Technology, University of Michigan, Ann Arbor, MI 48109

[3] G.M. Rebeiz, D.P. Kasilingam, Y. Guo, P.A.Stimson and D.B. Rutledge, "Monolithic millimeter-wave two-dimensional horn imaging arrays," IEEE Trans. on Antennas and Propagat. Vol. 38, pp. 1473-1482, Sep. 1990

[4] S.S. Gearhart and G.M. Rebeiz, "Integrated 119 ...m Corner Cube Antenans, " Submitted for publication in Applied Physics Letters, Dec. 1990

[5] V.D. Hwang, T. Uwano and T. Itoh, "Quasi-optical integrated antenna and receiver front end.", IEEE Trans. on Microwave Theory and Techniques, Vol. 36, No. 1, January 1988

[6] G. Elazar and M. Kisluik, "Microstrip linear slot array antenna for X-band.", IEEE Trans. on Antennas and Propagat. Vol. 36, pp. 1144-1147, Aud. 1988

[7] L. Rexberg, "Radiation from planar sources in layered dielectric media", Technical report No. 56L, School of Electrical and Computer Engineering, Chalmers University of Technology, Gothenburg, Sweden, November 1988.

[8] Roger F. Harrington, "Field Computation by Moment Methods", Macmillan Series in Electrical Science, The Macmillan Company, 1968

[9] D. R. Rhodes, "Synthesis of Planar Antenna Sources", Oxford University Press, Ely House, London W. 1, 1974

MISSING
PAGE

8 Appendix A: VSWR and reflection coefficient.

The voltage along any transmission line (Figure 34) can be written as a summation of two waves: one going in the positive x-direction ($V^+e^{-jk_x x}$) and one going in the negative x-direction ($V^-e^{+jk_x x}$). The sum of these two waves form a standing voltage wave as:

$$V(x) = V^+e^{-jk_x x} + V^-e^{+jk_x x} \tag{73}$$

or

$$V(x) = V^+\epsilon^{-jk_x x}(1 + \Gamma(0)e^{+j2k_x x}) \tag{74}$$

where $\Gamma(0)$ is the reflection coefficient at the load plane. We can define a voltage standing wave ratio by taking the ratio of the maximum voltage to the minimum voltage. The minimum and maximum voltages are evaluated as follows:

$$|V(x)| = |V^+\epsilon^{-jk_x x} + V^-e^{+jk_x x}| = |V^+||1 + \Gamma(0)e^{+j2k_x x}| \tag{75}$$

The maximum occurs when the phase of the reflection coefficient is zero and the minimum occurs when the phase is $-180°$ which gives:

$$|V(x)|_{max} = |V^+|(1 + |\Gamma(0)|) \tag{76}$$

$$|V(x)|_{min} = |V^+|(1 - |\Gamma(0)|) \tag{77}$$

from the maximum and minimum voltages be obtain the voltage standing wave ratio (VSWR) as:

$$\text{VSWR} = S = \frac{V(x)_{\max}}{V(x)_{\min}} = \frac{1 + |\Gamma(x)|}{1 - |\Gamma(x)|} = \frac{1 + |\Gamma(0)|}{1 - |\Gamma(0)|} \tag{78}$$

where:

$$\Gamma(x) = \frac{V^- e^{+jk_x x}}{V^+ e^{-jk_x x}} = \Gamma(0) e^{+j2k_x x} \tag{79}$$

or the reflection coefficient at the load plane can be written as:

$$\Gamma(0) = \Gamma(x)\, e^{-j2k_x x} \tag{80}$$

so, if the magnitude of the reflection coefficient is calculated at a maximum (at $x = -d$) to the left of the load, we get the reflection coefficient at the load plane as:

$$\Gamma(0) = \Gamma(-d)\, e^{+j2k_x d} \tag{81}$$

The input impedance at the load plane is then easily obatined from the reflection coefficient by the following relation:

$$\Gamma(0) = \frac{Z_L - Z_0}{Z_L + Z_0} \tag{82}$$

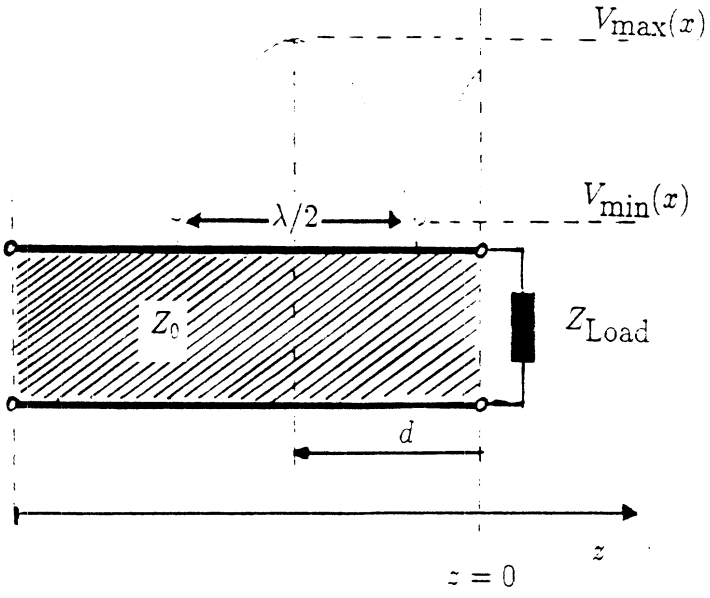

Figure 34: The standing wave pattern on a ideal transmission line. The reflection coefficient is obtained from the maxima and minima of the current or voltage.